Scribble, Lgl1, and myosin II form a complex in vivo to promote directed cell migration

Maha Abedrabbo and Shoshana Ravid*
Department of Biochemistry and Molecular Biology, The Institute of Medical Research Israel-Canada, The Hebrew University-Hadassah Medical School, Jerusalem 91120, Israel

ABSTRACT Scribble (Scrib) and Lethal giant larvae 1 (Lgl1) are conserved polarity proteins that play important roles in different forms of cell polarity. The roles of Scrib and Lgl1 in apical-basal cell polarity have been studied extensively, but little is known about their roles in the cell polarity of migrating cells. Furthermore, the effect of Scrib and Lgl1 interaction on cell polarity is largely unknown. In this study, we show that Scrib, through its leucine-rich repeat domain, forms a complex in vivo with Lgl1. Scrib also forms a complex with myosin II, and Scrib, Lgl1, and myosin II colocalize at the leading edge of migrating cells. The cellular localization and the cytoskeletal association of Scrib and Lgl1 are interdependent, as depletion of either protein affects its counterpart. In addition, depletion of either Scrib or Lgl1 disrupts the cellular localization of myosin II. We show that depletion of either Scrib or Lgl1 affects cell adhesion through the inhibition of focal adhesion disassembly. Finally, we show that Scrib and Lgl1 are required for proper cell polarity of migrating cells. These results provide new insights into the mechanism regulating the cell polarity of migrating cells by Scrib, Lgl1, and myosin II.

INTRODUCTION

Cell polarity is essential for various biological processes in different cell types, including cell migration, proliferation, differentiation, asymmetric division, tissue morphogenesis, and tumor formation (Zhu et al., 2014). Loss of cell polarity leads to tissue disorganization, uncontrolled proliferation, and migration, which are hallmarks of epithelial cancers (Martin-Belmonte and Perez-Moreno, 2012). Cell polarity is tightly regulated by the orchestration of three main conserved protein complexes, Scribble (Scrib), PAR, and Crumbs (Martin-Belmonte and Perez-Moreno, 2012). The Scrib module proteins play key functions in the establishment and maintenance of different modes of cell polarity, as well as in the control of tissue growth and differentiation, and therefore are important regulators

of tissue development and homeostasis (Humbert et al., 2006). The Scrib complex is composed of the Scrib, Lethal giant larvae (Lgl), and Discs large (Dlg) proteins. In Drosophila, homozygous mutants in these genes resulted in the loss of apico-basal cell polarity and neoplastic tissue overgrowth, identifying these proteins as tumor suppressors as well as polarity proteins (Bilder et al., 2000). In mammalians, Scrib, Lgl, and Dlg play tumor suppressive roles in epithelial cancers (Elsum et al., 2012). The similarity in the mutant phenotypes of Scrib, Dlg, and Lgl, and the genetic interactions between them have led to the assumption that they function in a common pathway to regulate the establishment and maintenance of different forms of cell polarities, such as apico-basal polarity in epithelial cells (Humbert et al., 2008).

Scrib is a membrane-associated protein that contains 16 leucine-rich repeats (LRRs) at its N-terminal and four PDZ domains at its C-terminal (Bonello and Peifer, 2019) (Figure 1A). Scrib is identified as a cell-junction-localized protein, essential for embryonic polarization and tumor suppression in Drosophila (Bilder et al., 2000; Bilder and Perrimon, 2000). Scrib overexpression in mammary epithelial cells suppresses the epithelial to mesenchymal transition and promotes epithelial differentiation (Elsum et al., 2013). Loss of Scrib disrupts epithelial cell polarity and contributes to mammary tumorigenesis (Zhan et al., 2008), suggesting that Scrib is a tumor suppressor in mammals. Scrib is frequently amplified and overexpressed in multiple human cancers (Pearson et al., 2011; Martin-Belmonte and Perez-Moreno, 2012). It has been suggested that proper membrane
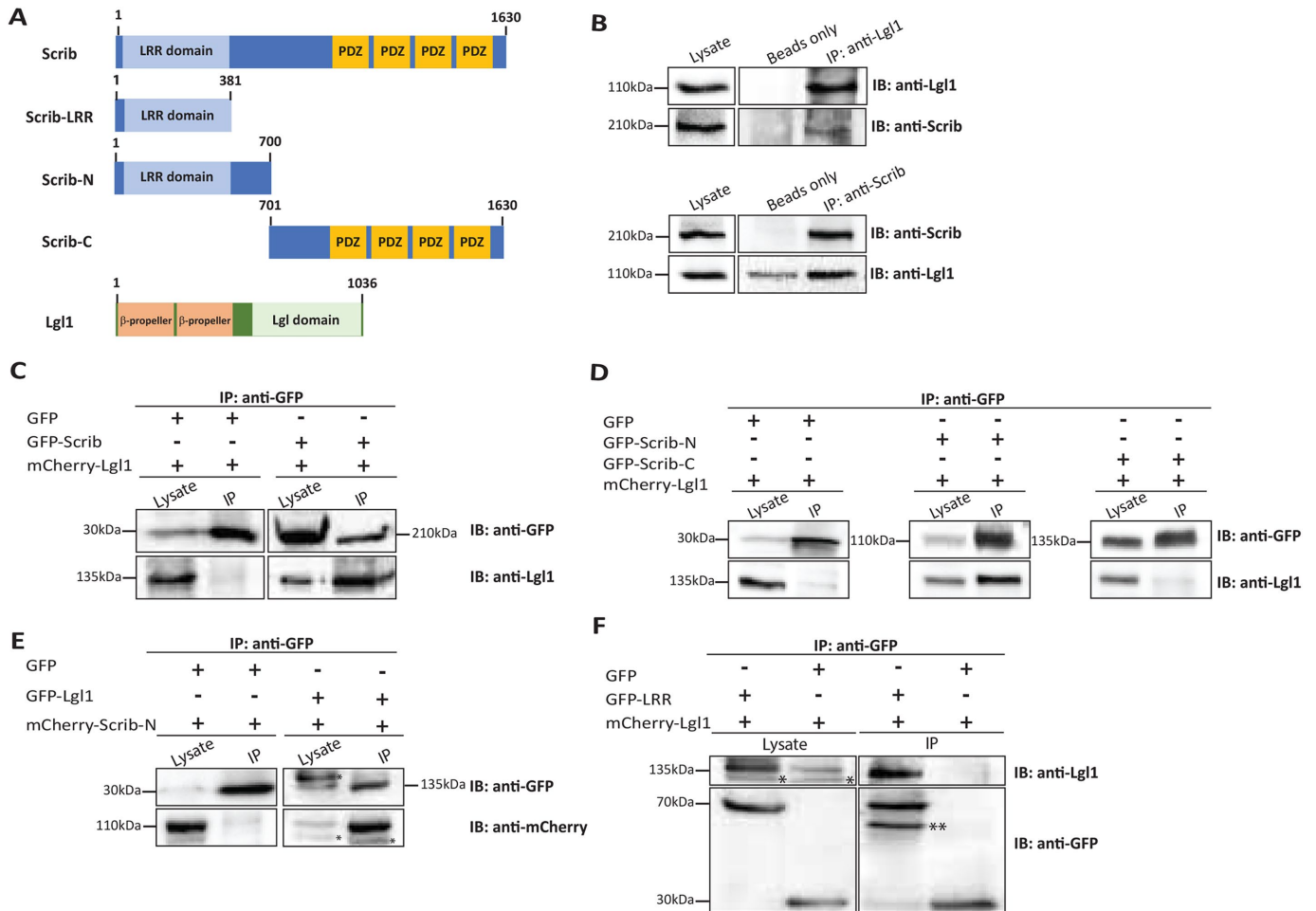
FIGURE 1: Lgl1 and Scrib interact through Scrib-LRR domain. (A) A schematic illustration of Scrib and Lgl1 proteins used in this study. (B) MDA-MB-231 cell extracts were subjected to immunoprecipitation assay using Lgl1 or Scrib antibodies. The immunoprecipitated proteins were analyzed by immunoblotting (IB) with antibodies against Scrib and Lgl1. Beads only were used as negative control. (C) mCherry-Lgl1, GFP-Scrib, or GFP-only, expressed in HEK293T cells subjected to coimmunoprecipitation (co-IP) assay using GFP antibody. The immunoprecipitated proteins were analyzed by IB with antibodies against GFP and Lgl1. GFP only was used as a negative control. (D) mCherry-Lgl1, GFP-Scrib-N, GFP-Scrib-C, or GFP-only, expressed in HEK293T cells and subjected to co-IP assay using GFP antibody. The immunoprecipitated proteins were analyzed by IB with antibodies against GFP and Lgl1. GFP only was used as a negative control. (E) mCherry-Scrib-N, and GFP-Lgl1 or GFP-only, expressed in HEK293T cells and subjected to co-IP assay using GFP antibody. The immunoprecipitated proteins were analyzed by IB with antibodies against GFP and mCherry. *Nonspecific bands. (F) mCherry-Lgl1 and GFP-LRR or GFP-only, expressed in HEK239T cells subjected to co-IP assay using GFP antibody. The immunoprecipitated proteins were analyzed by IB with antibodies against mCherry and GFP. GFP only was used as a negative control. *Endogenous Lgl1, **Nonspecific band. Molecular weight of the proteins are indicated.

localization of Scrib is essential for its tumor-suppressive activities, as flies with a mislocalized Scrib variant phenocopy the Scrib-deficient mutant (Zhan *et al.*, 2008; Feigin *et al.*, 2014). In addition to its roles in the different forms of cell polarity, Scrib also acts in diverse cell types as an important integrator of signals required to promote cell migration. In many of these cases, Scrib regulates Rho GTPase gradients to drive the front-to-back polarization required for directed cell migration activity (Osmani *et al.*, 2006; Dow *et al.*, 2007). For example, in astrocytes, Scrib recruits β-PIX, a guanine-nucleotide exchange factor, to the leading edge to facilitate localized Cdc42 activity (Osmani *et al.*, 2006). Similarly, in response to directional cues, MCF-10A epithelial cells require Scrib to recruit Rac1 and Cdc42 to the leading edge to form stable lamellipodial protrusions (Dow *et al.*, 2007).

Lgl consists of two domains: the N-terminal domain, which consists of two β-propellers serving as a docking platform for protein-protein interactions, and the C-terminal domain, which is Lgl specific (Figure 1A). There are two mammalian Lgl homologues, Lgl1 and Lgl2. Lgl1 is widely expressed, whereas Lgl2 has a more restricted expression pattern in mouse tissues (Klezovitch *et al.*, 2004). Loss of Lgl1 in mice results in the formation of neuroepithelial rosette-like structures, similar to the neuroblastic rosettes in human primitive neuroectodermal tumors (Klezovitch *et al.*, 2004). The expression of Lgl1 is strongly reduced in several tumor cell lines (Schimanski *et al.*, 2005; Kuphal *et al.*, 2006). Lgl is phosphorylated by atypical protein kinase C isoform ζ (aPKCζ); this phosphorylation regulates Lgl1 cellular localization, which is important for the correct polarity of migrating cells (Plant *et al.*, 2003; Dahan *et al.*, 2014). Scrib and Lgl interact with each

other genetically (Bilder *et al.*, 2000), but there is no evidence that Scrib and Lgl interact directly, although Lgl2 coimmunoprecipitates with Scrib in HEK293T and MDCK cells (Kallay *et al.*, 2006).

Biochemical and genetic analyses indicate that Lgl is the component of the cytoskeleton that interacts with nonmuscle myosin II (NMII), an interaction regulated by the phosphorylation of Lgl (Strand *et al.*, 1994a,b; Betschinger *et al.*, 2005; Dahan *et al.*, 2012, 2014). NMII is an actin-based motor protein that is important for cell migration through its effects on adhesion, lamellar protrusion, rear retraction, and polarity (Conti and Adelstein, 2008; Vicente-Manzanares *et al.*, 2009b). NMII is a hexamer composed of two heavy chains and two pairs of essential and regulatory light chains. The heavy chains include the α-helical coiled-coil rod domain responsible for the assembly of NMII monomers into filaments, the functional structures required for NMII activity. NMII filament formation is highly dynamic and regulated by phosphorylation (Murakami *et al.*, 2000; Dulyaninova *et al.*, 2005; Even-Faitelson and Ravid, 2006; Rosenberg and Ravid, 2006; Ronen and Ravid, 2009). Mammalian cells express three different NMII isoforms: NMIIA, NMIIB, and NMIIC (Shohet *et al.*, 1989; Simons *et al.*, 1991; Golomb *et al.*, 2004). In migrating fibroblasts, the NMII isoforms play different roles in cell polarity. NMIIA is dynamic and assembles actomyosin bundles in protrusions. By contrast, NMIIB incorporates into preformed F-actin bundles and remains stationary, defining the center and rear of the migrating cell, and mediates retraction of the trailing edge during migration (Vicente-Manzanares *et al.*, 2009b). NMIIB was shown to be important for increase of cancer stem cell invasion, whereas NMIIA was required for generating traction forces during initial adhesion and spreading (Thomas *et al.*, 2015). We have shown that Lgl1 interacts directly with NMIIA, regulating the polarity of migrating cells by controlling the assembly state of NMIIA, its cellular localization, and focal adhesion assembly (Dahan *et al.*, 2012). The Lgl1-NMIIA interaction is regulated by aPKCζ phosphorylation of Lgl1 (Dahan *et al.*, 2014).

The roles of Scrib and Lgl1 in apical-basal cell polarity has been studied extensively, but little is known about their roles in polarity of migrating cells. The functions of Scrib and Lgl1 in cell polarity have been studied for each protein individually, and the effect of their interaction on cell polarity in general, as well as on the polarity of migrating cells, is largely unknown. In this study, we show that Scrib and Lgl1 form a complex in vivo through the Scrib-LRR domain. Scrib also forms a complex with NMIIB, and Scrib, Lgl1, and NMIIB colocalize at the leading edge of migrating cells. Depletion of Lgl1 or Scrib disrupts the cellular localization and the cytoskeletal association of Scrib and Lgl1, respectively, as well as of NMIIB. Finally, we show that the complex formation of Scrib and Lgl1 is required for the proper polarity of migrating cells, cell migration, and adhesion.

RESULTS

Scrib and Lgl1 form a complex in vivo

The idea that Scrib, Lgl, and Dlg form a complex derives from the observations that in *Drosophila*, mutations in these genes produce similar phenotypes, and the proteins show complete or partial colocalizations, which are interdependent (Bilder *et al.*, 2003; Tanentzapf and Tepass, 2003; Bilder, 2004). It was also reported that Lgl2, the less abundant Lgl isofrom, coimmunoprecipitates with Scrib (Kallay *et al.*, 2006). These studies prompted us to investigate whether Lgl1 and Scrib interact biochemically in mammalian cells and to characterize these interactions. To this end, we tested whether endogenous Scrib and Lgl1 reside in a complex in MDA-MB-231 cells. For this purpose, Scrib or Lgl1 were immunoprecipitated and the coimmunoprecipitated proteins were analyzed. As shown in Figure 1B,

Scrib was coimmunoprecipitated with Lgl1 and the reciprocal experiment further indicated that Lgl1 forms a complex with Scrib (Figure 1B).

To determine the Scrib domain that interacts with Lgl1, we first coexpressed GFP-Scrib and mCherry-Lgl1 in HEK293T cells and preformed a coimmunoprecipitation assay. GFP-Scrib, but not GFP, coimmunoprecipitated with mCherry-Lgl1, attesting to the specificity of Lgl1 and Scrib interaction (Figure 1C). Next, we coexpressed in HEK293T cells the N-terminal domain of Scrib (GFP-Scrib-N, amino acids (aa) 1–700) or the C-terminal domain of Scrib (GFP-Scrib-C, aa 701–1630) (Figure 1A) with mCherry-Lgl1. Extracts obtained from these cell lines were subjected to coimmunoprecipitation assay. As shown in Figure 1D, GFP-Scrib-N but not GFP-Scrib-C coimmunoprecipitated with mCherry-Lgl1. The reciprocal experiment further indicated that Lgl1 forms a complex with Scrib-N (Figure 1E). To map more precisely the Scrib domain that forms a complex with Lgl1, we created GFP-Scrib-LRR (aa 1–381, Figure 1A) and coexpressed it with mCherry-Lgl1 in HEK293T cells. The coimmunoprecipitation assay indicated that Lgl1 forms a complex with Scrib through its LRR domain (Figure 1F). Note that most of the known Scrib-interacting proteins interact with Scrib through its C-terminal domain (Stephens *et al.*, 2018; Wen and Zhang, 2018). Thus, the complex formation of Scrib-Lgl1 may point to a unique role for this protein complex.

Pull-down assays using recombinant purified Scrib and Lgl1 proteins failed to indicate a direct interaction between these proteins (data not shown). Together, these results indicate that Scrib and Lgl1 form a complex in vivo, and that this interaction is mediated by other protein(s).

Scrib and Lgl1 form distinct complexes

Lgl1 forms a multiprotein polarity complex with Par6 and aPKCζ (Plant *et al.*, 2003; Dahan *et al.*, 2014), indicating an intercomplex regulation between the Scrib module and the Par complex (Wen and Zhang, 2018). We have previously demonstrated that Lgl1 interacts directly with aPKCζ and that the complex Lgl1-Par6-aPKCζ resides in the leading edge of migrating cells (Dahan *et al.*, 2014). To further understand the interaction between the Scrib and the Par polarity complexes in migrating cells, we tested whether aPKCζ also resides in the Scrib-Lgl1 complex. We found that GFP-Lgl1 but not with GFP-Scrib coimmunoprecipitated with endogenous aPKCζ (Figure 2A). These results indicate that in the cell, the polarity protein Lgl1 resides in discrete protein complexes, Lgl1-Scrib and Lgl1-aPKCζ, respectively (Figure 2K).

Cell polarity during cell migration is important to distinguish random cell migration, in which cells migrate in all directions in a noncoordinated manner, from directed cell migration, in which cells respond to polarizing cues to migrate in a given direction. In both cases, cell polarity is required to generate a front-rear axis (Ridley *et al.*, 2003). NMII plays different roles in the cell polarity of migrating cells (Vicente-Manzanares *et al.*, 2009a). We have shown that Lgl1 exists in a complex with NMIIA, which regulates its cellular localization in polarized migrating cells (Dahan *et al.*, 2012). Given the important role of NMII in cell migration and invasion (Vicente-Manzanares *et al.*, 2008, 2011; Thomas *et al.*, 2015), we tested whether endogenous NMIIA or NMIIB interact with endogenous Scrib or Lgl1 in MDA-MB-231 cells. To this end, we preformed immunoprecipitation of endogenous NMIIA or NMIIB and examined the presence of endogenous Lgl1 and Scrib in these complexes. We found that NMIIA formed a complex with Lgl1 but not with Scrib, while NMIIB formed a complex with Scrib but not with Lgl1 (Figure 2B and Supplemental Figure S1A). Similar results were obtained when GFP-Lgl1 or GFP-Scrib were coimmunoprecipitated
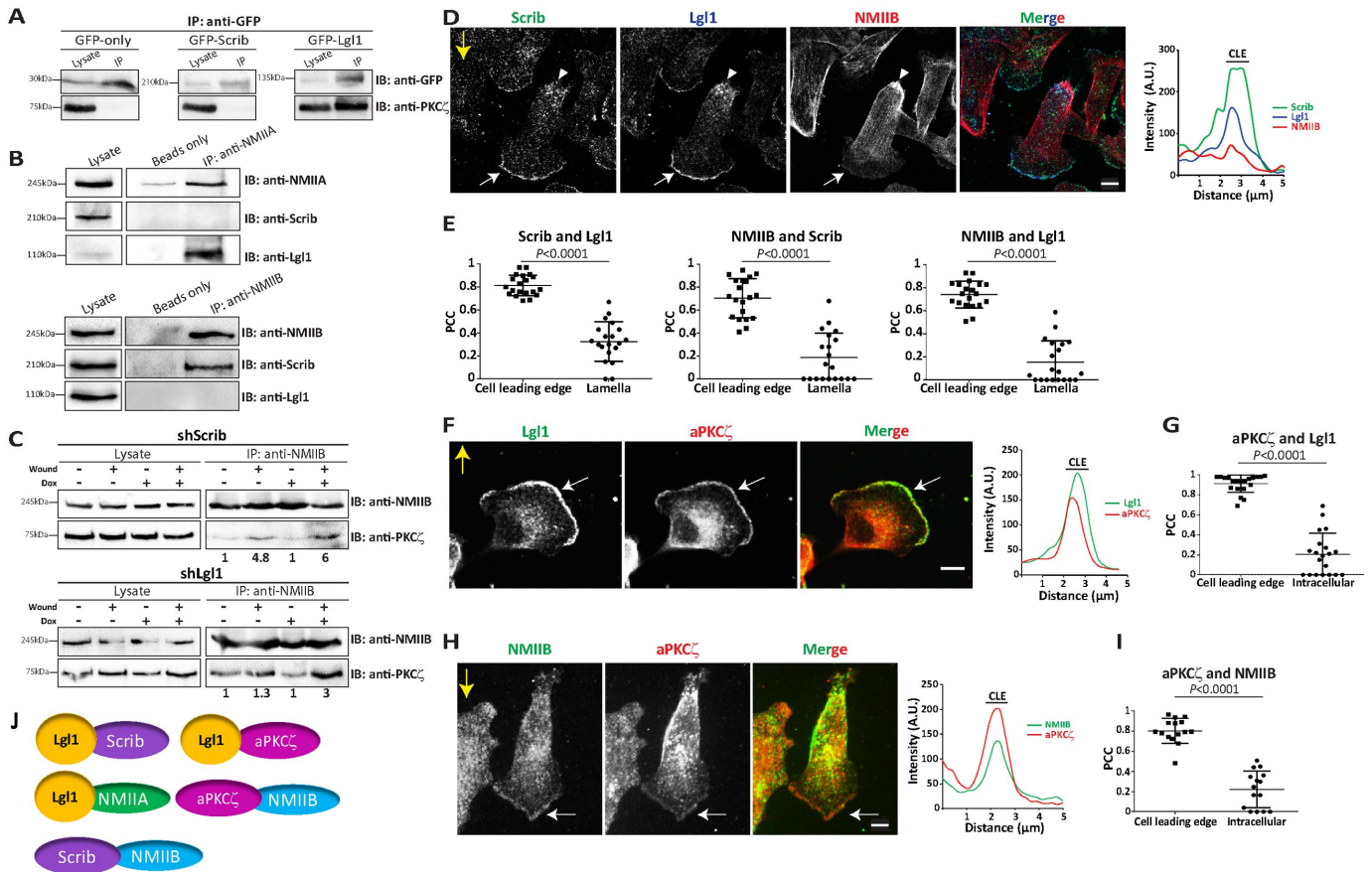
FIGURE 2: Scrib and Lgl1 form distinct protein complexes in mammalian cells. (A) GFP-Scrib, GFP-Lgl1, or GFP-only, expressed in HEK293T cells subjected to co-IP assay with endogenous aPKCζ using GFP antibody. The immunoprecipitated proteins were analyzed by IB with antibodies against GFP and aPKCζ. (B) MDA-MB-231 cell extracts were subjected to IP assay using NMIIA or NMIIB antibody. The immunoprecipitated proteins were analyzed by IB with antibodies against NMIIA, NMIIB, Scrib, and Lgl1. Beads only were used as negative control. (C) MDA-MB-231 cells depleted for Lgl1 and Scrib, shLgl1, and shScrib cell lines, respectively, were treated with or without Dox, subjected to wound scratch assay followed by IP using NMIIB antibody. The immunoprecipitated proteins were analyzed by IB with antibodies against NMIIB and aPKCζ. The numbers below the gel lanes represent the relative amount of aPKCζ associated with NMIIB, which was determined from the band intensity using ImageGauge software, and normalized relative to the samples obtained from untreated control cells. Molecular weights of the protein are indicated. (D, F, H) Cellular localization of Scrib, Lgl1, NMIIB, and aPKCζ. MDA-MB-231 cells were subjected to wound scratch assay, fixed, and immunostained for Scrib, Lgl1, and NMIIB (D); for Lgl1 and aPKCζ (F); and for NMIIB and aPKCζ (H). Scale bar, 10 µm. Yellow arrows indicate direction of migration and white arrows indicate that localization of Scrib, Lgl1, aPKCζ, and NMIIB to the cell leading edge. The fluorescent intensity was measured 1 µm outside of the cell leading edge and 5 µm toward the cell center. (E, G, I) PCC between the fluorescence intensity of endogenous Scrib, Lgl1, and NMIIB (E); Lgl1 and aPKCζ (G); and NMIIB and aPKCζ (I) at the cell leading edge and in the lamella. Cell leading edge was defined as the outer rim of the front of the cell that is highlighted by the staining of Scrib, Lgl1, NMIIB, or aPKCζ. The lamella was defined as the region behind the cell outer rim. Results are mean ± SD, n = 20, 20, and 15, respectively, subjected to paired Student's t test. (J) A model depicting the different complexes that are formed by Lgl1, Scrib, NMIIA, NMIIB, and aPKCζ at the cell leading edge.

with endogenous NMIIB (Supplemental Figure S1B). Thus, Lgl1 forms a complex with NMIIA and Scrib with NMIIB.

We have previously shown that NMIIB resides in a complex with p21-activated kinase (PAK1) and aPKCζ, and that the interaction between these proteins is a cue-signal-dependent mechanism (Even-Faitelson and Ravid, 2006). We further showed that aPKCζ phosphorylates NMIIB directly in a cue-signal-dependent manner, affecting NMIIB filament assembly and its cellular localization (Even-Faitelson and Ravid, 2006). Next, we tested whether Scrib or Lgl1 affects the aPKCζ-NMIIB complex formation in cells subjected to wound scratch assay as a signal cue. To this end, we created MDA-MB-231 cells depleted of Scrib or Lgl1 using two different methods,

both equally efficient in reducing the expression of Scrib and Lgl1 (Supplemental Figure S2, A and B). Note that the expression levels of Lgl1 in Scrib-depleted cells and of Scrib in Lgl1-depleted cells were not affected (Supplemental Figure S2, A and B). Scrib- or Lgl1-depleted cell lines were subjected to wound scratch assay, and the aPKCζ-NMIIB complex formation was analyzed with a coimmuno-precipitation assay. Stimulation of control cells with wound scratch led to increased amounts of aPKCζ that were associated with NMIIB compared with unstimulated cells (Figure 2C). The amounts of aPKCζ that were associated with NMIIB were further enhanced by the depletion of Scrib or Lgl1 (Figure 2C). Quantification of the relative amounts of aPKCζ associated with NMIIB further indicated that

shScrib and shLgl1 cell lines untreated with Dox were increased by 4.8- and 1.3-fold on stimulation with wound scratch (Figure 2C). On depletion of Scrib or Lgl1, the association was further increased to six- and threefold (Figure 2C) repectively. Thus, the aPKCζ-NMIIB complex formation is enhanced by an extracellular directional migration cue, indicating that aPKCζ regulates NMIIB in migrating cells. Because aPKCζ binds Lgl1 and NMIIB binds Scrib, on depletion of Lgl1 and Scrib, there is an increase in free aPKCζ and NMIIB, respectively, which may increase the amounts of aPKCζ associated with NMIIB.

To further explore the role of the Scrib-Lgl1 complex in polarized migrating cells, we characterized the cellular localization of these proteins in MDA-MB-231 cells subjected to wound scratch assay to achieve polarized migrating cells. In polarized migrating MDA-MB-231 cells, endogenous Scrib and Lgl1 mainly colocalized at the cell leading edge (Figure 2D). Some of the Scrib and Lgl1 proteins were also localized at the rear part of the cells. These observations were confirmed by quantification of the fluorescence intensity of Scrib and Lgl1 from the leading edge of the cell toward its center (Figure 2D). The fluorescence intensity patterns of Scrib and Lgl1 were similar with maximum fluorescence at the cell edge (Figure 2D). To analyze the level of Scrib and Lgl1 colocalization, the Pearson correlation coefficient (PCC) was calculated between the fluorescence intensity profiles of Scrib and Lgl1 in the cell leading edge compared with the lamella (Figure 2E). Quantitatively, the PCC between Scrib and Lgl1 in the cell leading edge (0.81 ± 0.09; mean ± SD) was significantly higher than in the lamella (0.33 ± 0.17). Thus, Scrib and Lgl1 colocalize at the cell leading edge. These results are consistent with the findings that Scrib is recruited to the leading edge of migrating astrocytes (Osmani *et al.*, 2006), and that Lgl1 colocalized with F-actin at the cell leading edge of migrating fibroblasts (Plant *et al.*, 2003; Dahan *et al.*, 2012). Next, we analyzed the cellular localization of endogenous NMIIB. We found that NMIIB localized mainly at the rear of the cell and was associated with stress fibers, as described previously (Kolega, 1998; Gupton and Waterman-Storer, 2006; Vicente-Manzanares *et al.*, 2011). Some of NMIIB colocalized with Scrib and Lgl1 at the cell leading edge (Figure 2D). These observations were confirmed by quantification of the fluorescence intensity of NMIIB, Scrib, and Lgl1 from the leading edge of the cell toward its center (Figure 2D). The fluorescence intensity patterns of NMIIB, Scrib, and Lgl1 were similar with maximum fluorescence at the cell leading edge (Figure 2D). Similarly, the PCC between Scrib and NMIIB and Lgl1 and NMIIB in the cell leading edge (0.7 ± 0.17 and 0.74 ± 0.11, respectively) was significantly higher than in the lamella (0.27 ± 0.17 and 0.15 ± 0.15, respectively) (Figure 2E).

The localization of NMIIB at the cell leading edge is in contrast to the known cellular localization of NMIIB that is absent from the cell leading edge of migrating cells such as CHO-K1 and fibroblasts (Vicente-Manzanares *et al.*, 2007, 2008). Yet, it has been shown that in MDA-MB-231 cells, NMIIB is recruited to the lamellar margin during active spreading on fibronectin, and that NMIIB seems to play a role in the mechanics of lamellar protrusion (Betapudi *et al.*, 2006). NMIIA was also found to concentrate at the cell leading edge (Figure 3C). Thus, in MDA-MB-231 cells, NMII isoforms are localized at the cell leading edge, in addition to their known cellular localization. Next, we tested the cellular localization of aPKCζ, Lgl1, and NMIIB in MDA-MB-231 cells migrating cells. We found that aPKCζ concentrated along with Lgl1 and NMIIB at the cell leading edge and some of it was cytoplasmic (Figure 2, F and H). These observations were confirmed by quantification of the fluorescence intensity of these proteins from the leading edge of the cell toward its center as well as by PCC quantification between aPKCζ and Lgl1 and between

aPKCζ and NMIIB (Figure 2, F–I). Quantitatively, the PCC between aPKCζ and Lgl1 or NMIIB in the cell leading edge (0.91 ± 0.08 and 0.80 ± 0.12, respectively) was significantly higher than in the lamella (0.21 ± 0.21 and 0.22 ± 0.18, respectively). These results further indicate that the complexes Lgl1-aPKCζ and NMIIB-aPKCζ are formed at the cell leading edge.

Together, these results indicate that several distinct complexes are formed within the cell, Scrib-Lgl1, Scrib-NMIIB, Lgl1-NMIIA, as well as Lgl1-aPKCζ and NMIIB-aPKCζ (Figure 2J).

The cellular localization of Scrib and Lgl1 is interdependent

To test the effect of the Scrib-Lgl1 interaction on their cellular localization, cells lines depleted of Scrib or Lgl1 were subjected to wound scratch assay, and the cellular localization of Scrib, Lgl1, and NMIIB was examined. In cells depleted of Scrib, Lgl1 was diffused mainly within the cells, and was missing from the leading edge of the cells, unlike control cells, in which Lgl1 was localized mainly at the cell leading edge and some of it at the rear part of the cells (Figure 3A). Similarly, Scrib in cells depleted of Lgl1 was diffused in the cell body and missing from the cell leading edge, in contrast to control cells, in which Scrib was localized in the cell leading edge and some of it in the cell body (Figure 3B). These observations indicate that Lgl1 and Scrib are important for the cell leading edge localization of Scrib and Lgl1, respectively. Thus, the cellular localization of Scrib and Lgl1 in the cell leading edge is interdependent. Because Scrib forms a complex with NMIIB, we tested whether Scrib or Lgl1 affects the spatial segregation of NMIIB during cell migration. To this end, cells depleted of Scrib or Lgl1 were subjected to wound scratch assay and immunostained for NMIIB. In cells depleted of Scrib or Lgl1, NMIIB was absent from the lamellipodium and was diffused throughout the cells, in contrast to control cells, in which NMIIB was localized at the rear of the cells and at the cell leading edge (Figure 3, A and B). These results indicate that the Scrib-Lgl1 complex plays a role in the proper cellular localization of NMIIB. Next, we tested how the absence of Lgl1 or Scrib affects the cellular localization of NMIIA. For this purpose, the cellular localization of NMIIA was examined in cells depleted of Scrib or Lgl1 and subjected to wound scratch assay. We found that NMIIA localized at the cell leading edge and in the cytoplasm (Figure 3C). On Lgl1 depletion the width of the cell leading edge that was occupied by NMIIA was significantly higher than that in control cells (2.91 ± 0.79 and 1.67 ± 0.56, respectively). In contrast, depletion of Scrib did not affect the amounts of NMIIA localized at the cell leading edge (1.77 ± 0.56 and 1.59 ± 0.55) (Figure 3D). These results are consistent with our previous findings that in fibroblasts NMIIA is missing from the cell leading edge presumably because the inhibitory effect of Lgl1 on NMIIA filament assembly and depletion of Lgl1 results in the presence of NMIIA in this region (Dahan *et al.*, 2012). In addition, these results may indicate that Scrib or Lgl1 affects the cellular localization of NMIIA and NMIIB in different manner.

To further study the effect of Scrib-Lgl1 interaction on their cellular localization, we determined the amounts of Scrib and Lgl1 associated with the cytoskeleton in Lgl1- and Scrib-depleted cells, respectively, using a (TX-100) solubility assay. In a control cell line subjected to wound scratch assay, most of Scrib (82%) was associated with the cytoskeleton, and depletion of Lgl1 resulted in a significant decrease in the amounts of Scrib (56%) associated with the cytoskeleton (Figure 3E), indicating that Lgl1 contributes to the cytoskeletal association of Scrib. Thirty percent of Lgl1 was associated with the cytoskeleton in control cells, and depletion of Scrib resulted in a significant decrease in Lgl1 association with the cytoskeleton (10%) (Figure 3F). These results indicate that similarly to Scrib, Lgl1
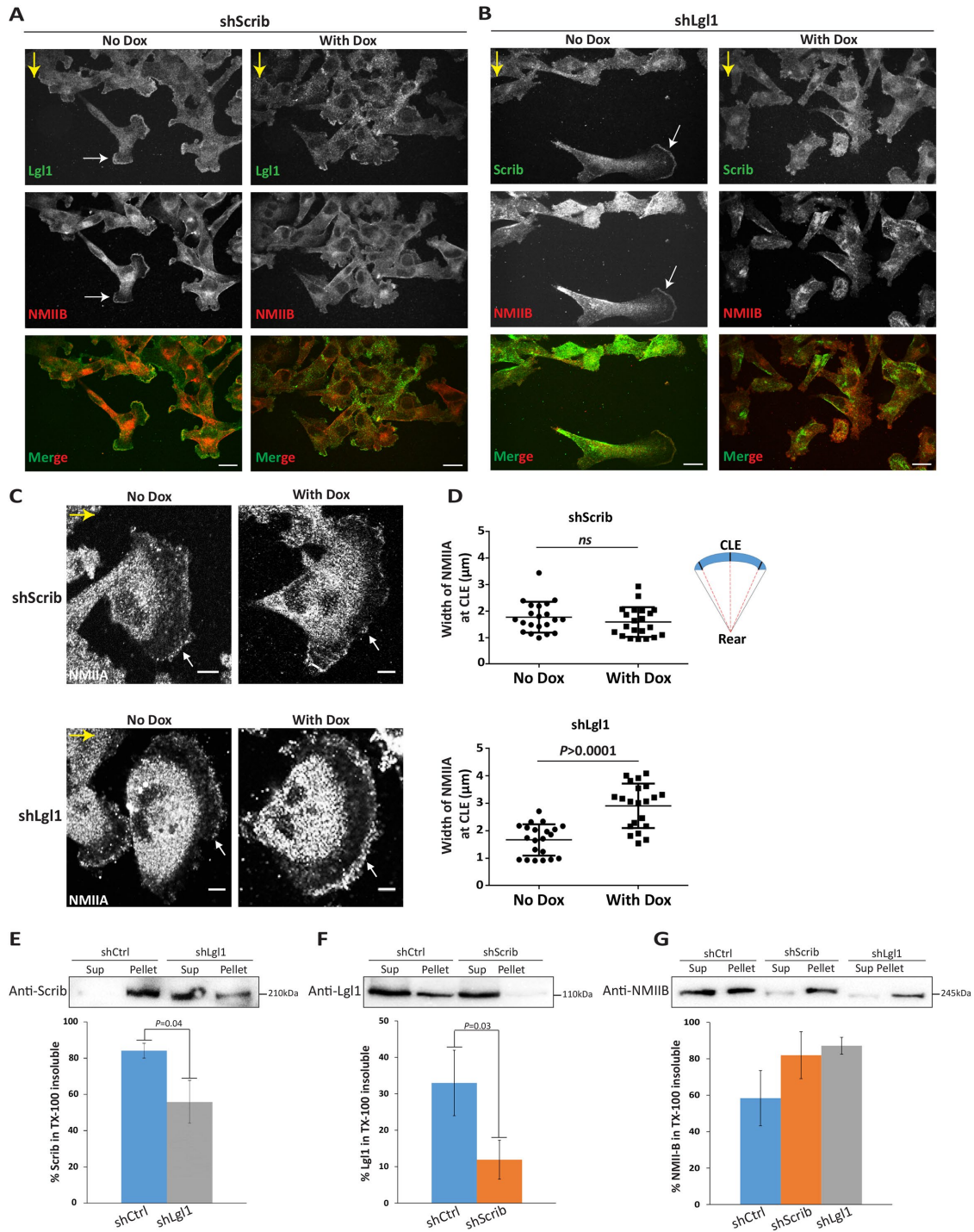
FIGURE 3: Cellular localization of Scrib and Lgl1 is interdependent. shScrib (A) and shLgl1 (B) cell lines with or without Dox were subjected to wound scratch assay, fixed, and immunostained for Scrib, Lgl1, and NMIIB. Yellow arrows indicate the direction of migration and white arrows indicate that localization of Scrib, Lgl1, and NMIIB to the cell leading edge. Scale bar, 20 µm. (C) shScrib and shLgl1 cell lines with or without Dox were subjected to wound scratch assay, fixed, and immunostained for NMIIA. Yellow and white arrows indicate the direction of migration and the localization of NMIIA to the cell leading edge, respectively. Scale bar, 10 µm. (D) The width of the cell leading edge occupied by NMIIA was determined by averaging three regions (black lines) along the cell leading edge (CLE) of each cell stained for NMIIA as described in the diagram. Data represent the mean ± SD from $n = 20$ subjected to two-tailed, two-sample, and unequal-variance Student's t test; ns, not significant. (E–G) shCtrl, shScrib, and shLgl1 cell lines were subjected to TX-100 solubility assay. Lgl1, Scrib, and NMIIB in the TX–100-soluble (Sup) and in the TX–100-insoluble (Pellet) fractions were analyzed with IB using antibodies to Scrib (E), Lgl1 (F), and NMIIB (G). The percentage of Lgl1, Scrib, and NMIIB in the Triton-insoluble fractions was determined. Values are the mean ± SD from three independent experiments subjected to two-tailed, two-sample, and unequal-variance Student's t test. Molecular weights of the proteins are indicated.

cytoskeletal association is affected by the presence of Scrib and is consistent with the immunostaining results (Figure 3B). A higher percentage of NMIIB was associated with the cytoskeleton on depletion of either Scrib or Lgl1 (81% and 87% vs. 56% in control cells; Figure 3G). These data indicate that in the absence of Scrib or Lgl1, higher amounts of NMIIB are associated with the cytoskeleton. These results may indicate that Scrib has an inhibitory effect on NMIIB filaments assembly, similar to the inhibitory effect that Lgl1 has on the NMIIA filament assembly (Dahan *et al.*, 2012). Although NMIIB does not interact with Lgl1, depletion of Lgl1 led to higher amounts of NMIIB associated with the cytoskeleton and to aberrant cellular

localization. We propose that Lgl1 does not affect NMIIB directly, but rather through its effects on Scrib. In other words, in the absence of Lgl1, Scrib exhibits aberrant cellular localization and cytoskeletal association, affecting the behavior of NMIIB. Together, these results indicate an interactive complex involving Lgl1-Scrib-NMIIB.

Scrib and Lgl1 are required for proper cell adhesion

In the course of characterizing the Scrib- and Lgl1-depleted cells, we noticed that these cell lines adhered more firmly than control cells. Indeed, adhesion assay indicated that cells depleted of Scrib or Lgl1 were ~1.6- and ~1.3-fold more adhesive than the control cell
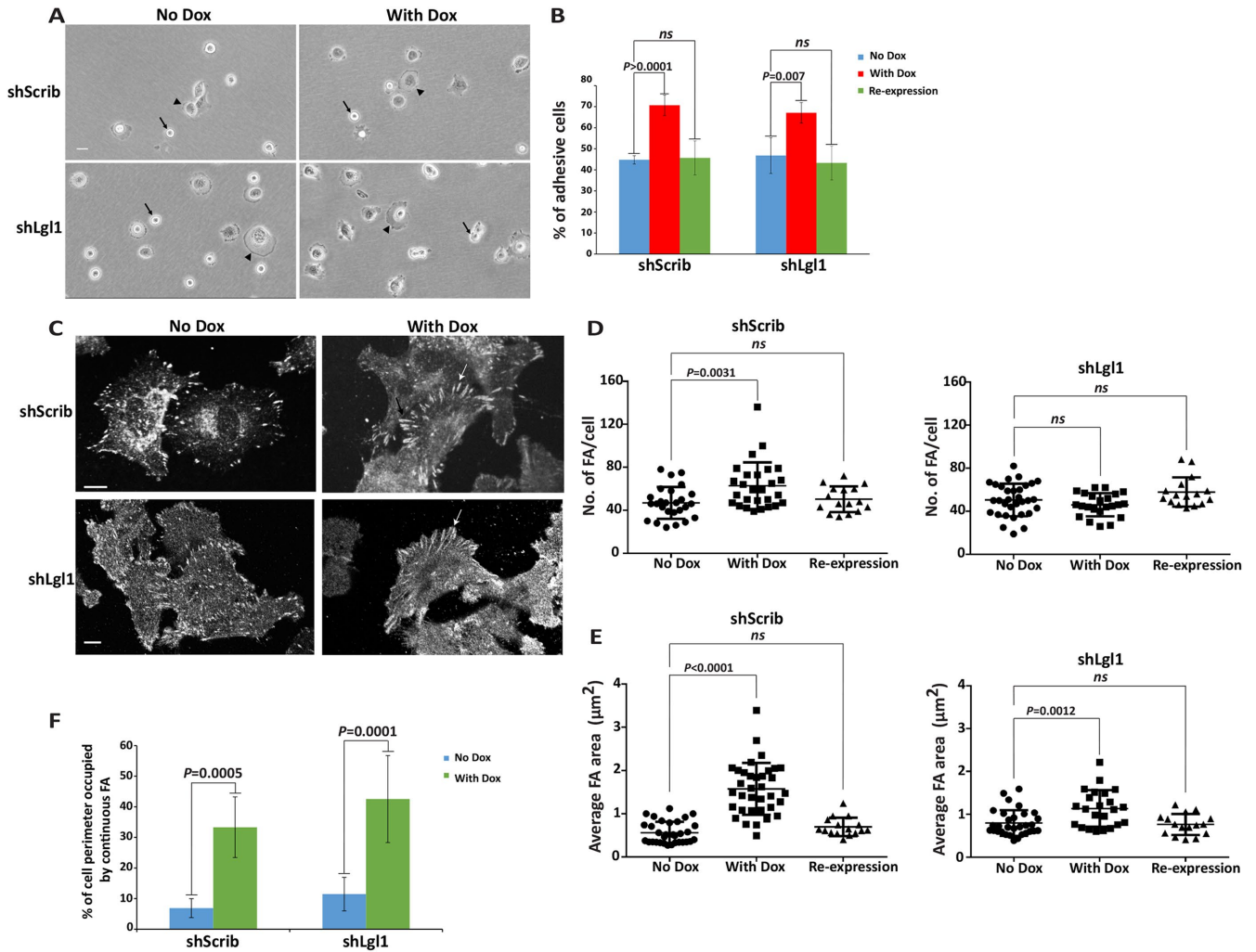

FIGURE 4: Scrib and Lgl1 play a role in cell adhesion. (A) shScrib and shLgl1 cell lines with or without Dox were seeded on dishes, and after 45 min, phase-contrast images of the cells were taken by confocal microscopy. Arrows and arrowheads indicate nonadhesive and adhesive cells, respectively. Scale bar, 10 µm. (B) Quantification of adhered cells in shScrib and shLgl1 treated with or without Dox and in shLgl1 and shScrib cell lines treated with Dox and expressing Neon-Lgl1 and Neon-Scrib, respectively. Adhered and rounded detached cells in 10 randomly chosen fields were counted and the percentage of adhered cells in each field was calculated. Values are the mean ± SD from three independent experiments, subjected to ANOVA with a post hoc test; ns, not significant. (C) shScrib and shLgl1 cell lines with or without Dox were subjected to wound scratch assay, fixed, and immunostained for Paxillin. Arrows indicate large focal adhesions. Scale bar, 10 µm. (D) Dot-plot of average number of focal adhesion (FA) per cell in shScrib cell line, n = 31 (no Dox), n = 28 (with Dox), shLgl1 cell line n = 43 (no Dox), n = 33 (with Dox), and cells depleted for Scrib or Lgl1 expressing Neon-Scrib (n = 16) and Neon-Lgl1 (n = 16), respectively. Values are the mean ± SD subjected to ANOVA with a post hoc test. (E) Dot-plot of the average focal adhesion size per cell in shScrib cell line, n = 32 (no Dox), n = 32 (with Dox), shLgl1 cell line, n = 43 (no Dox), n = 33 (with Dox), and in cells depleted for Scrib or Lgl1 expressing Neon-Scrib (n = 16) and Neon-Lgl1 (n = 16), respectively. Values are the mean ± SD subjected to ANOVA with a post hoc test. (F) Quantifications of the percentage of cell perimeter occupied by large FA. shScrib cell line, n = 7 (no Dox), n = 9 (with Dox), and shLgl1 cell line, n = 7 (no Dox), n = 10 (with Dox). Values are the mean ± SD subjected to ANOVA with a post hoc test.

line (Figure 4, A and B). Similar observations were reported following the depletion of Lgl1 from fibroblast (Dahan *et al.*, 2012). To address the specificity of Scrib and Lgl1 shRNA, we tested whether the effects of Scrib and Lgl1 depletion could be rescued with re-expression of Scrib or Lgl1 which are resistant to the shRNA targeting Scrib or Lgl1 (Supplemental Figure S2C). The shRNA was targeted to the 3′ untranslated region (UTR) of Scrib or Lgl1 and this allowed us to re-express Scrib or Lgl1 from cDNA clones that did not contain the 3′ UTR. Re-expression of Scrib or Lgl1 in cells depleted for Scrib or Lgl1, respectively, decreased the percentage of adhesive cells to the levels of control cells (Figure 4B).

Several studies have shown the involvement of NMII and Lgl1 in cell adhesion. Depletion of NMII decreases the size of adhesions (Vicente-Manzanares *et al.*, 2008; Parsons *et al.*, 2010), underscoring the requirement for NMII activity in maintaining these structures. Depletion of Lgl1 from fibroblast promoted small, nascent focal adhesions, indicating that Lgl1 is involved in focal adhesion maturation, possibly through the regulation of NMIIA (Dahan *et al.*, 2012). These studies prompted us to examine the role of Scrib and Lgl1 in focal adhesion morphology and formation in MDA-MB-231 cells. To this end, cells depleted of Scrib or Lgl1 were immunofluorescently stained for paxillin as focal adhesion marker (Figure 4C), and the number of focal adhesions per cell was determined. Depletion of Scrib resulted in an increase in the number of focal adhesion per cell (46 vs. 61 focal adhesions/cell) (Figure 4D). By contrast, depletion of Lgl1 did not affect significantly the number of focal adhesions per cell (control, 50 vs. shLgl1 46 focal adhesions/cell) (Figure 4D). Re-expression of Scrib and Lgl1 in cells depleted for Scrib and Lgl1, respectively, restored the number of focal adhesion to control levels (Figure 4D). Next, we analyzed the focal adhesion size in cells depleted of Scrib or Lgl1. Depletion of Scrib led to a significant increase in the average size of focal adhesions, compared with control cells (0.56 ± 0.25 vs. 1.57 ± 0.58 μm^2) (Figure 4E). Similarly, depletion of Lgl1 led to a significant increase in the average size of focal adhesion (0.8 ± 0.3 vs. 1.14 ± 0.42) (Figure 4E). Re-expression of Scrib or Lgl1 in cells depleted for Scrib and Lgl1, respectively, reduced the size of focal adhesion to control levels (0.6 ± 0.2 and 0.76 ± 0.24, respectively) (Figure 4E). At cell–cell junctions, control cells as well as cells depleted of Scrib or Lgl1 exhibited large focal adhesions (~10 μm^2). The phenomenon was robust in cells depleted of Scrib or Lgl1 (Supplemental Figure S3A). Thus, Scrib and Lgl1 may play a role in focal adhesion disassembly. We also noticed that some of the cells depleted of Scrib or Lgl1 presented continuous focal adhesions, mainly at the cell leading edge, ranging between 17 and 35 μm^2 (Supplemental Figure S3B). We found that ~6% of the cells depleted of Scrib had continuous focal adhesions that occupied ~33% of the cell perimeter compared with 2% of control cells with continuous focal adhesions that occupied ~11% of the cell perimeter (Figure 4E). This phenomenon was even more robust in cells depleted of Lgl1: ~15% of cells depleted of Lgl1 had ~43% of their perimeter occupied with large focal adhesions compared with 2% of control cells, which had ~13% of their perimeter occupied with continuous focal adhesion. These results may indicate that Scrib and Lgl1 are involved in the disassembly process of focal adhesions. In the absence of Scrib or Lgl1, focal adhesion disassembly is perturbed, leading to cells with large focal adhesions and high adhesive properties.

Depletion of Scrib or Lgl1 impairs cell polarity in migrating cells
Because Scrib and Lgl1 play important roles in the polarity of migrating cells (Osmani *et al.*, 2006; Dahan *et al.*, 2012; Michaelis

et al., 2013), we tested how depletion of Scrib or Lgl1 affects the polarity of migrating cells. MDA-MB-231 cells subjected to wound scratch assay presented three distinct cell morphologies (Figure 5A). We quantified these morphologies to provide a polarity index (PI). The index is the result of dividing the length of the main migration axis, which denotes the direction of migration, by the length of the perpendicular axis that passes through the center of the nucleus. Cells with a PI smaller than 1 exhibited a wide lamella and a short rear end, resulting in a crescentlike shape (Figure 5A); cells with a PI between 1 and 3.5 had the classic front-rear migrating cell morphology; and cells with a PI higher than 3.5 had an elongated morphology (Figure 5A). The different cell morphologies are an indication of the extent of cell contractility, with a PI < 1 and >3.5 representing low and high contractility, respectively. Depletion of either Scrib or Lgl1 led to a significant decrease in cells with a PI between 1 and 3.5 and a significant increase in cells with a PI > 3.5 (Figure 5, B and C). These cells had an elongated shape, indicating loss of cell polarity and impairment in the formation of the cell rear, a role previously ascribed to NMIIB (Vicente-Manzanares *et al.*, 2008). Because Scrib regulates NMIIB association with the cytoskeleton (Figure 3E), and Lgl1 regulates the assembly state of NMIIA (Figure 3C and Dahan *et al.*, 2012), we propose that in the absence of either Lgl1 or Scrib, NMIIA and NMIIB exhibit filament overassembly, leading to high cell contractility and elongated cell morphology. Thus, Scrib and Lgl1 affect the architecture of the actomyosin network in the cell cortex regulating cortical contractility and cell polarity.

In addition to differences in cell morphology, the position of the nucleus and the Golgi apparatus are also the hallmarks of migratory cell polarization. The Golgi apparatus reposition in front of the nucleus toward the direction of protrusion (Nabi, 1999; Etienne-Manneville and Hall, 2001). To further understand the role of Scrib and Lgl1 in establishing cell polarity in migrating cells, we analyzed the orientation of the Golgi complex in cells depleted of Scrib or Lgl1 and subjected to wound scratch assay (Figure 5D). Depletion of Scrib or Lgl1 led to a significant decrease in the percentage of cells whose Golgi apparatus was oriented in the direction of migration, 39% and 43%, respectively, compared with control cells (~57%) (Figure 5E). Re-expression of Scrib or Lgl1 in cells depleted for Scrib and Lgl1, respectively, increased the percentage of cells with the correct orientation to control levels (~53%) (Figure 5E). Together, these results indicate that Scrib and Lgl1 play an important part in the establishment of front-rear cell polarity in migrating cells.

Scrib and Lgl1 are essential for directed cell migration
Having observed the defects in the cell polarity of migrating cells on Scrib or Lgl1 depletion, we next determined the effect of Scrib and Lgl1 depletion on directed cell migration. To this end, we assessed the ability of cells depleted of Scrib or Lgl1 to initiate migration in a wound scratch assay. In contrast to control cells that migrated in one sheet to close the wound, some of the Scrib- or Lgl1-depleted cells detached from the cell sheet and moved in different directions, as single cells or as a group of a few cells (Figure 6A). Next, we determined the ability of the Scrib- or Lgl1-depleted cells to close a wound. Whereas control cells closed ~65% of the wound 15 h after wounding, cells depleted of Scrib or Lgl1 closed only ~40% and ~30% of the wound, respectively (Figure 6C).

To further understand the role of Scrib and Lgl1 on directed cell migration, we tracked single-cell migration using time-lapse microscopy of cells depleted of Scrib or Lgl1 and subjected to wound scratch assay. We derived the persistence of migration (the ratio of the vectorial distance traveled to the total path length of the cell) and
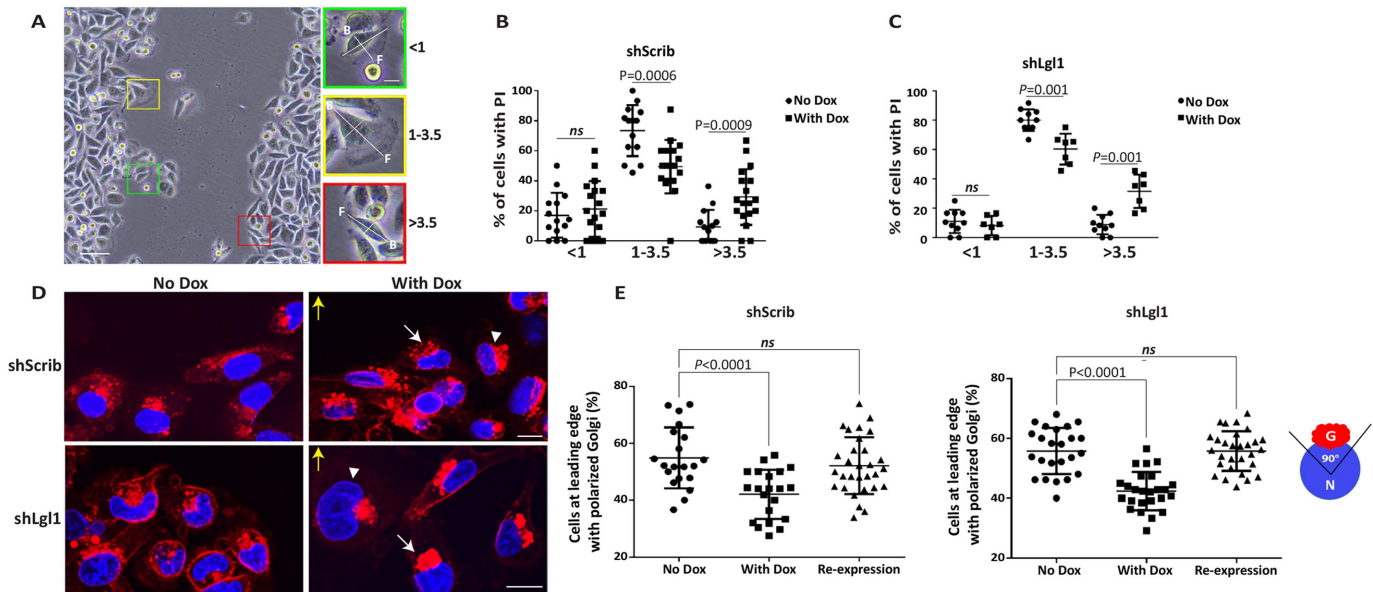
FIGURE 5: Scrib and Lgl1 depletion disrupt cell polarity. (A) A representative image of cells in wound. Scale bar, 50 µm. The colored boxes indicate the different forms of cell polarity, and their respective PIs are indicated to the right. White lines indicate the axes used to calculate the PI. F, Front; B, Back; scare bar, 8 µm. shScrib (B) and shLgl1 (C) cell lines with or without Dox were subjected to wound scratch assay and images were taken 4 h after the wound and the PI distribution of the cells in the first row along the wound edge was determined. Data represent the percentage of cells in each field exhibiting the different PI, shscrib cell line 14 fields, $n = 129$ (without Dox), 18 fields, $n = 158$ (with Dox), and shLgl1 cell line 10 fields, $n = 107$ (without Dox), 7 fields, $n = 107$ (with Dox). Values are the mean ± SD subjected to two-tailed, two-sample, and unequal-variance Student's t test. (D) shScrib and shLgl1 cell lines with or without Dox were subjected to wound scratch assay and nuclei and Golgi apparatus were stained. Yellow arrow indicates the direction of migration. White arrows and arrowheads indicate correctly and incorrectly oriented cells, respectively. Scale bar, 20 µm. (E) Quantification of the percentage of wound-edge cells with their Golgi apparatus in the quadrant that is in front of their nucleus and facing the wound (blue-red diagram) is presented in Dot-plot. N, Nucleus; G, Golgi apparatus. Data represent the mean ± SD of $n > 480$ cells at least from 20 fields subjected to ANOVA with a post hoc test; ns, not significant.

cell speed from the track plots. Whereas control cells moved along relatively straight paths, with high persistence of migration, cells depleted of Scrib or Lgl1 moved randomly, with several changes in direction, some of them moving in circles returning to their starting point (Figure 6D). These cells also demonstrated a significant decrease in persistence (shScrib, 0.27 and shLgl1, 0.24) compared with control cells (0.69) (Figure 6E). Furthermore, the migration rate of Scrib- and Lgl1-depleted cells was lower than that of control cells (1.02 and 1.08 vs. 3.17 µm/h) (Figure 6F). Because the rate of cell migration is determined by the turnover of focal adhesions, we propose that in the absence of Scrib or Lgl1, there is slower focal adhesions disassembly affecting cell speed and persistence.

DISCUSSION

Using biochemical assays, we showed that Scrib, through its LRR domain, forms a complex with Lgl1 in vivo. Repeated attempts to detect a direct interaction between Scrib and Lgl1 failed; therefore, we can state with a high degree of confidence that these proteins do not interact directly, and there is another protein(s) that mediates the interaction between Scrib and Lgl1, similar to the adaptor protein Guk-holder, which is necessary to physically couple Scrib with Dlg (Mathew et al., 2002; Caria et al., 2018). Proteomics approaches identified protein complexes that involved Scrib and Lgl1 (Daulat et al., 2018; Pires and Boxem, 2018), and we will use such approaches to identify the protein(s) that links Scrib to Lgl1. Because mutations in Scrib and Lgl1 produce identical phenotypes, and the

proteins show complete or partial colocalizations, it was suggested that Scrib and Lgl1 perform their functions in cell polarity when they are in a complex (Bilder et al., 2000). Note, however, that Scrib and Lgl1 also function independently of each other (Daulat et al., 2018). For example, mutation in Scrib did not affect collective migration, whereas mutation in Lgl triggered invasion (Szafranski and Goode, 2007). Therefore, Scrib and Lgl1 may perform related but separate functions, as components of distinct protein complexes in the different forms of cell polarity.

Scrib and Lgl1 are indispensable for the establishment and maintenance of epithelial cell polarity (Assemat et al., 2008), but the mechanism by which Scrib and Lgl1 contribute to the establishment of polarity in migrating cells is poorly understood. Our data contribute to the understanding of this mechanism. We show that in addition to the association of Scrib with Lgl1, the two are also associated with NMII, Scrib is associated with NMIIB, and Lgl1 with NMIIA (Dahan et al., 2012). Furthermore, aPKCζ is associated with Lgl1 but not with Scrib, and aPKCζ is also associated with NMIIB that is enhanced in response to extracellular directional cues, such as wound healing (in this study), and EGF (Even-Faitelson and Ravid, 2006). We propose that in response to extracellular migration cues, such as a chemotactic gradient, or during wound healing, several protein complexes are formed: Scrib-Lgl1, Scrib-NMIIB, Lgl1-NMIIA, aPKCζ-Lgl1, and aPKCζ-NMIIB (Figure 2K). These protein complexes colocalize at the leading edge of migrating cells and together promote cell polarity and directed cell migration. The cellular
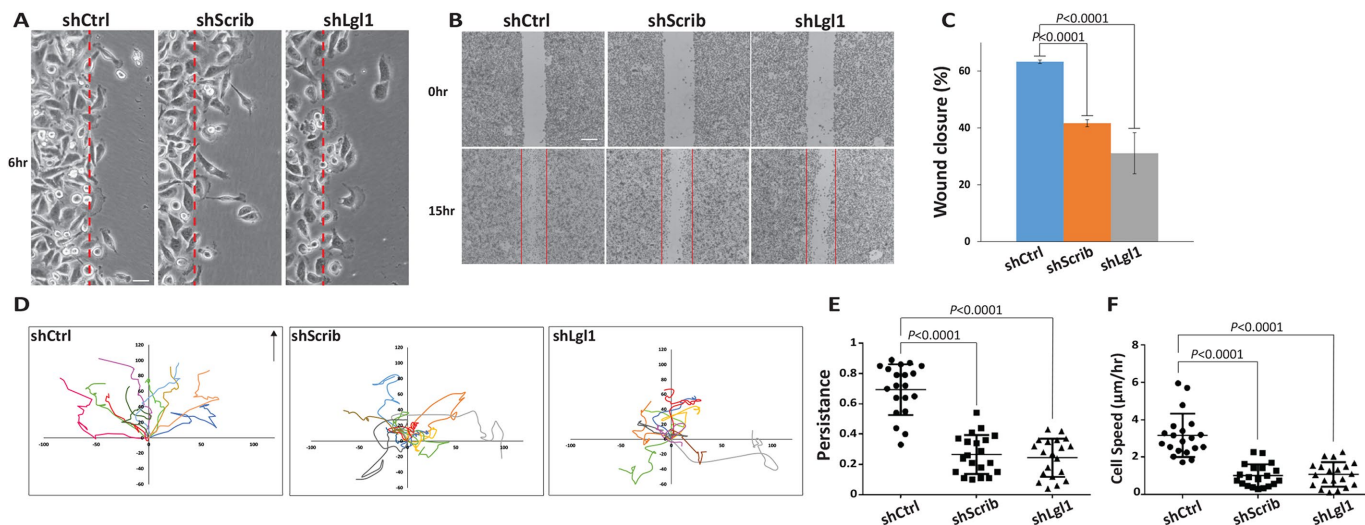
FIGURE 6: Scrib and Lgl1 regulate directed cell migration. (A, B) shCtrl, shScrib, and shLgl1 cell lines were subjected to wound scratch assay and images were taken at the start of the experiment (0 h), 6 h later (6 h) and 15 h later (15 h) as indicated. Dashed lines indicate the edge of the wound and solid lines indicate the boundary of the wound at 0 h. Scale bars, 500 and 50 µm, respectively. (C) Wound rate closure at 15 h. Values are the mean ± SD from three independent experiments subjected to ANOVA with a post hoc test. (D) shCtrl, shScrib, and shLgl1 cell lines were seeded on µ-Slide 4 well-coated chamber and subjected to wound scratch assay; cells were tracked using time-lapse confocal microscopy at 30-min intervals. The paths of 10 randomly chosen cells were plotted for each experimental group. Paths are oriented in such a way that the start point is normalized to the origin. The persistence of migration (E) and the speed of migration (F) were extracted from the track plots and presented in dot-plot. Persistence is defined as the ratio of the vectorial distance traveled to the total path length described by the cell. Values are the mean ± SD for $n > 20$ from two independent experiments subjected to ANOVA with a post hoc test.

localization of Scrib and Lgl1 in the lamellipodium of migrating cells, as well as their cytoskeletal association, are interdependent. It was reported that the LRR domain of Scrib facilitates correct localization of Scrib at the cell membrane (Bonello and Peifer, 2019). Because the Scrib-LRR domain forms a complex with Lgl1, we propose that Scrib and Lgl1 localization at the cell leading edge of migrating cells requires the Scrib-LRR domain. Thus, in the absence of either Scrib or Lgl1, neither of these proteins localized properly in migrating cells. In addition, Lgl1 binds to the plasma membrane and to NMII containing cytoskeleton through its C-terminal domain (Dahan et al., 2012; Bailey and Prehoda, 2015; Dong et al., 2015). Scrib and Lgl1 affect the cellular localization and the cytoskeletal association of NMIIB and NMIIA. We propose that the Scrib-Lgl1 complex is anchored to the plasma membrane as well as to the cytoskeleton through interaction with NMIIA and NMIIB. The increased amounts of cytoskeletal NMIIB in cells depleted of Scrib may indicate that Scrib negatively regulates NMIIB cytoskeletal association. Similarly, depletion of Lgl1 increased the amounts of NMIIA at the cell leading edge, thus Lgl1 regulates the cellular localization of NMIIA by binding to NMIIA, inhibiting its filament assembly (Dahan et al., 2012, 2014). Hens, Scrib, and Lgl1 may regulate the amounts of NMIIA and NMIIB localized at the cell leading edge, balancing between actin polymerization and NMIIA and NMIIB filament assembly, which are required for lamellipodial extension and cell migration. Although Lgl1 does not form a complex with NMIIB, the amounts of NMIIB associated with the cytoskeleton increase on depletion of Lgl1. We propose that the effect of Lgl1 on NMIIB is indirect, exercised through the effect of Lgl1 on Scrib. The increase of cytoskeletal NMIIB may also explain the other defects in cell adhesion, polarity, and migration exhibited by cells depleted of Scrib or Lgl1. Thus, in migrating cells, Scrib and Lgl1 are involved in several mechanisms that promote cell polarity (Figure 7A). Scrib is fre-

quently amplified and overexpressed in multiple human cancers (Pearson et al., 2011; Martin-Belmonte and Perez-Moreno, 2012), contrary to its tumor-suppressive functions in genetic studies. It has been suggested that proper membrane localization of Scrib is essential for its tumor-suppressive activities (Feigin et al., 2014). We propose that the oncogenic properties of Lgl1 exhibited by cells with low Lgl1 expression can be also related to Scrib mislocalization.

Another level of regulation of cell polarity of migrating cells is provided by aPKCζ. We show that aPKCζ forms discrete complexes with Lgl1 and NMIIB, and colocalizes with these proteins at the leading edge of migrating cells. aPKCζ phosphorylates Lgl1 in a region that interacts with the plasma membrane (Moreira and Morais-de-Sa, 2016), regulating the cellular localization of Lgl1 (Dahan et al., 2014). aPKCζ also phosphorylates NMIIB heavy chains in response to directional cues regulating its cytoskeletal association (Even-Faitelson and Ravid, 2006). We propose that NMIIB phosphorylation by aPKCζ regulates its cytoskeletal association as well as its association with Scrib at the cell leading edge. Thus, in migrating cells, aPKCζ phosphorylates Lgl1 and NMIIB, regulating their localization at the cell leading edge (Figure 7B).

NMII plays a main role in directed cell migration. NMIIA is enriched anteriorly, and NMIIB coassembles with NMIIA filaments and becomes the dominant isoform in the posterior of the cell to promote polarized migrating cells (Kolega, 1998; Vicente-Manzanares et al., 2008; Raab et al., 2012). NMIIB also plays an important role in migratory cell polarization by positioning the nucleus during migration (Lo et al., 2004; Gomes et al., 2005). Furthermore, NMIIA promotes maturation and turnover of lamella focal adhesions, while NMIIB promotes long-lived focal adhesions in the cell center and rear (Vicente-Manzanares et al., 2011). Depletion of either Scrib or Lgl1 led to an increase in focal adhesion size, and we propose that
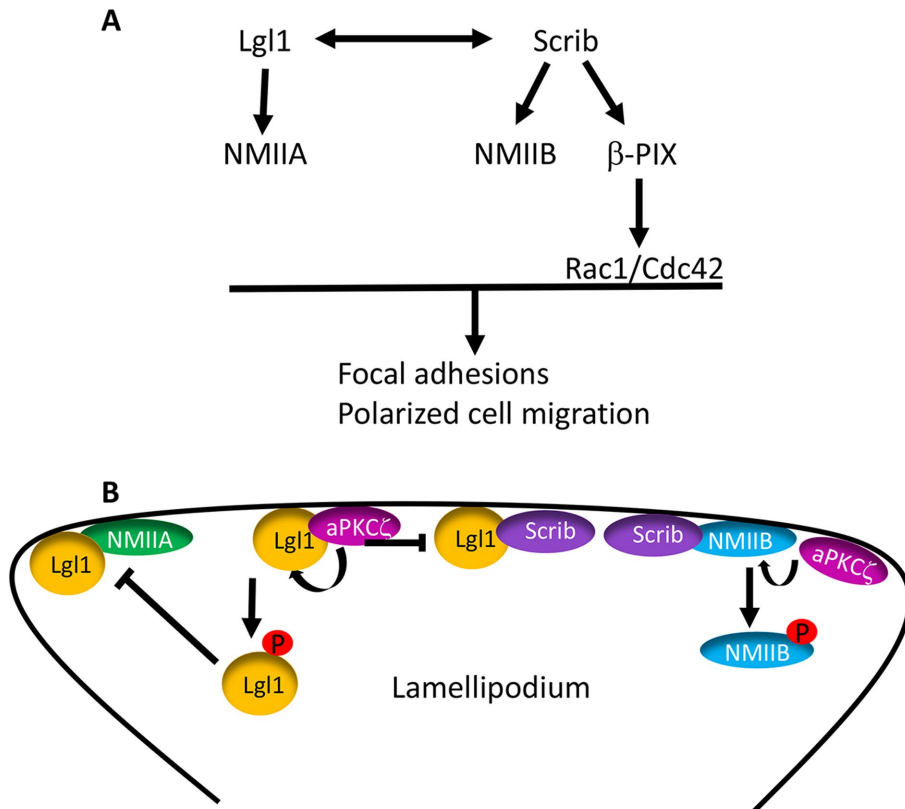
FIGURE 7: The different roles of Scrib and Lgl1 in polarized cell migration. (A) Lgl1 and Scrib affect polarized cell migration together in a complex as well as independent of each other. Lgl1-Scrib complex promotes cell polarity by localizing at the cell leading edge. In addition, Lgl1 and Scrib affect the cellular localization of NMIIA and NMIIB, respectively. Scrib through interaction with β-PIX affects Rac1/Cdc42 activity as well as focal adhesion disassembly. Together Scrib, Lgl1, and NMII proteins function to promote polarized cell migration. (B) Scrib and Lgl1 binds to NMIIB and NMIIA, respectively, regulating their cellular localization at the cell leading edge through their effect on NMII filament assembly. aPKCζ phosphorylates Lgl1 inhibiting its binding to the cell membrane and to the NMIIA containing cytoskeleton. aPKCζ may also affect the Lgl1-Scrib complex formation by reducing the amounts of Lgl1 available at the cell membrane. Finally, aPKCζ phosphorylates NMIIB regulating its cytoskeletal association as well as its association with Scrib.

Scrib and Lgl1 affect the dynamic of focal adhesions maturation and turnover through regulation of the cellular localization of NMIIA and NMIIB (Figure 7A). We previously showed that depletion of Lgl1 from fibroblasts promotes small, nascent focal adhesions (Dahan et al., 2012). In the current study, we show that depletion of Lgl1 increases the number of large mature adhesions. In fibroblasts, NMIIA localizes outside of protrusions regulating maturation of nascent cell adhesions in the lamella. In contrast, in MDA-MB-231 cells, NMIIA localizes at the cell leading edge as well as at the rear of the cell. Thus, it is plausible that in MDA-MB-231 cells, NMIIA regulates focal adhesion dynamics and maturation at the cell leading edge. On depletion of Lgl1, the amounts of NMIIA accumulated at the cell leading edge increased significantly. We postulate that this increase leads to aberrant focal adhesion dynamics resulting in large focal adhesions.

Scrib regulates Rho GTPase gradients to drive the front-to-back polarization required for directed cell migration (Osmani et al., 2006; Dow et al., 2007; Frank and Hansen, 2008). Scrib directly binds to β-PIX, and it is required to anchor β-PIX at the cell cortex (Audebert et al., 2004). β-PIX activates Rac1 and Cdc42, for example, in astrocytes. Scrib recruits β-PIX to the leading edge to facilitate

localized Cdc42 activity (Osmani et al., 2006). Similarly, in response to directional cues, MCF-10A epithelial cells require Scrib to recruit Rac1 and Cdc42 to the leading edge to form stable lamellipodial protrusions (Dow et al., 2007). Fibroblasts and epithelial cells deficient in β-PIX move slower and exhibit a defect in directed cell migration (Audebert et al., 2004; Cau and Hall, 2005; ten Klooster et al., 2006; Nola et al., 2008; Yu et al., 2015). Furthermore, β-PIX is required for lamellipodial formation, cell shape changes, and Rac1 activity induced by inhibition of NMII (Kuo et al., 2011). We propose that Scrib affects cell migration through the β-PIX-Rac1/Cdc42 pathway (Figure 7A). Thus, in cells depleted of Scrib, β-PIX is not localized at the leading edge of migrating cells on directional cues, leading to the absence of Rac1 activation in that region and to inhibition of lamellipodial extension and cell migration. Therefore, Scrib affects polarized cell migration through regulation of β-PIX cellular localization, a mechanism that is independent of Lgl1.

Through β-PIX, Scrib may also affect focal adhesion dynamics (Figure 7A). Screening of the proteome of focal adhesions recovered Scrib as one of many proteins enriched in these complexes (Humphries et al., 2009). β-PIX also accumulates in assembling nascent adhesions in the absence of NMII contractility, and it dissociates from focal adhesions during NMII-mediated focal adhesion maturation (Kuo et al., 2011). In fibroblasts, astrocytes, and certain epithelial cells, β-PIX is a negative regulator of focal adhesion maturation (Zhao et al., 2000; Kuo et al., 2011), and loss of β-PIX inhibits focal adhesion disassembly (Kuo et al., 2011; Hiroyasu et al., 2017). Indeed, cells depleted for Scrib exhibit large continuous focal adhesions, and we propose that β-PIX in these cells is inactive, leading to aberrant focal adhesion dynamics because of the inhibition of focal adhesion disassembly. In addition to its role in Rho GTPase regulation, Scrib has also been shown to promote directed migration of endothelial cells by regulating the turnover of integrin α5 at focal adhesions (Michaelis et al., 2013).

MATERIALS AND METHODS
Cell culture and growth conditions
MDA-MB-231 and HEK293T cell lines were maintained in high glucose DMEM (Sigma-Aldrich) supplemented with 2 mM L-glutamine, 10% fetal calf serum, and antibiotics (100 U/ml penicillin, 100 mg/ml streptomycin, and 1:100 Biomyc3 anti-mycoplasma antibiotic solution; Biological Industries, Beit HaEmek, Israel). Cells were grown at 37°C in a humidified atmosphere of 5% CO_2 and 95% air.

Antibodies
Goat polyclonal and mouse monoclonal anti-human Scrib (sc-11049) and (sc-55532, sc-55543), respectively, and mouse monoclonal anti-aPKCζ (sc-17781) were from Santa Cruz Biotechnology. Antibodies

Primer	Sequence 5'–3'
1	GCA TCG AAT TCA TGC TCA AGT GCA TCC CGC TGT GG
2	GGT CGG ATC CCT AAG AAA CCA CGG CCC C
3	GCT CAG AAT TCG CGC CCT CTG TCA GGG GAG TTT CG
4	CCT GAG GAT CCC TAG GAG GGC ACA GGG CCC
5	GGA TCC TCA ATT GAG GTG GGT GAG CGC
6	GGC CGG AAT TCT AAT GC TCAA GTG CAT CCC G
7	TCA GCA GGA TCC ATG CTC AAG TGC ATC CCG
8	TCA GCA GGA TCC ATG ATG AAG TTT CGG TTC
9	CTT GGA TCC TCA GCC CAG AAA ATC CTT C

TABLE 1: Primers used for plasmid constructions.

specific for the N- and C-terminal region of Lgl1 were generated in rabbits (Dahan *et al.*, 2012). Recombinant GFP antibodies were prepared in rabbits (Rosenberg and Ravid, 2006). Mouse monoclonal β-actin antibody (A5441) was from Sigma-Aldrich. Antibodies specific for the C-terminal region of human NMIIA and NMIIB were generated in rabbits according to the method of (Phillips *et al.*, 1995). Mouse monoclonal anti-NMIIB (ab684) and rabbit polyclonal mCherry antibody (ab167453) were from Abcam. Mouse monoclonal anti-paxillin (P13520) was purchased from BD Transduction Laboratories. Rabbit polyclonal anti-Lgl1 (D2B5A) was from Cell Signaling Technology. Horseradish peroxidase–conjugated secondary antibodies, donkey anti-mouse conjugated to Rhodamine, donkey anti-goat conjugated to Alexa Fluor 488, and goat anti-rabbit conjugated to Cy5 were from Jackson ImmunoResearch Laboratories. All antibodies were diluted 1:1000 for Western blot and 1:100 for immunofluorescence.

Preparation of plasmids

All restriction enzymes were from New England Biolabs. All PCR reactions were preformed using KAPA HiFi PCR Kit (KAPA Biosystems) or Phusion High-Fidelity DNA polymerase (ThermoFisher Scientific) according to manufacturer instructions. Primers used for plasmid constructions are shown in Table 1. To create mCherry-Lgl1, pGFP-Lgl1 (Dahan *et al.*, 2012) was digested with *Bam*HI and the fragment was ligated into pm-Cherry plasmid digested with *Bam*HI. To create EGFP-Scrib-N (aa 1–700) and EGFP-Scrib-C (aa 701–1630), EGFP-Scrib was subjected to PCR with primers #1 and #2, #3 and #4, respectively. PCR fragments were digested with *Bam*HI and *Eco*RI, and the fragments were ligated into GFP-C2 plasmid digested with *Eco*RI and *Bam*HI. To create GFP-Scrib-LRR (1–381), GFP-Scrib-N was subjected to PCR with primers #1 and #5. The PCR fragment was digested with *Bam*HI and *Eco*RI and ligated into EGFP-C2 plasmid digested with *Eco*RI and *Bam*HI. To create mCherry-Scrib-N, GFP-Scrib-N was subjected to PCR with primers #6 and #2. The PCR fragment was digested with *Bam*HI and *Eco*RI and ligated into pm-Cherry digested with *Eco*RI and *Bam*HI. To create Tet-plko-shScrib and Tet-plko-shLgl1, oligonucleotides forward and reverse for both shScrib and shLgl1 (Table 2) were annealed to form dsDNA encoding shRNA sequences targeting Scrib and Lgl1, respectively. The dsDNA fragments were ligated into Tet-pLKO-puro (Addgene) digested with *Age*I and *Eco*RI. pLenti-neon was a gift from Alex Rouvinski's lab. To create Lenti-Neon-Scrib and Lenti-Neon-Lgl1, GFP-Scrib and GFP-Lgl1 were subjected to PCR with primers #7 and #4, #8 and #9, respectively. PCR fragments were digested with *Bam*HI and ligated into pLenti-neon plasmid digested with *Bam*HI.

Generation of Scrib and Lgl1 depletion cell lines

HEK293T cells grown to 90% confluency were transfected with pGag pol, pMPG-VSVG, and shScramble (TRC1/1.5 Sigma-Aldrich) or shScrib (TRCN0000004458 Sigma-Aldrich) or shLgl1 (TRCN0000117137 Sigma-Aldrich) using polyethylenimine (PEI). At 8 h posttransfection, the medium was replaced with fresh medium, and at 24 and 48 h posttransfection, the supernatant was collected. The supernatant was centrifuged for 30 min at 500 × *g*, filtered with a 0.45-mm filter, aliquoted, and used directly or stored at –80°C. MDA-MB-231 cells were infected with the viruses containing the shRNA-Scramble or shRNA-Scrib or shRNA-Lgl1; 24 h postinfection, the medium was replaced with fresh medium. At 48 h postinfection, fresh medium containing 2 μg/ml Puromycin (Sigma-Aldrich) was added. Knockdown of Scrib or Lgl1 was verified by Western blot.

Generation of inducible Scrib and Lgl1 depletion cell lines

HEK293T cells grown to 90% confluency were transfected with pRev, pPM2, pTat, pVSVG, and tet-pLKO-shScrib or tet-pLKO-shLgl1 using PEI; 8 h posttransfection, the medium was replaced with a fresh medium. At 24 and 48 h posttransfection, the supernatant was collected and filtered with a 0.45-μm filter, and 4 μg/ml Polybrene was added. MDA-MB-231 cells were infected with the viruses containing tet-pLKO-shscrib or tet-pLKO-shLgl1; 24 h postinfection, the medium was replaced with fresh medium and 48 h postinfection, fresh medium containing 2 μg/ml Puromycin (Sigma-Aldrich) was added to the infected and control cells. Once the control cells died, knockdown of Scrib or Lgl1 was induced with 1 μg/ml Dox; 95% of Scrib and Lgl1 knockdown was detected 72 and 24 h after Dox addition by Western blot (Supplemental Figure S2B).

Generation of rescue Neon-Scrib and Neon-Lgl1 cell lines

HEK293T cells grown to 90% confluency were transfected with pRev, pPM2, pTat, pVSVG, and Lenti-Neon-Scrib or Lenti-Neon-Lgl1 using PEI; 8 h posttransfection, the medium was replaced with a fresh medium. At 24 and 48 h posttransfectio, the supernatant was collected and filtered with a 0.45 μm filter, and 4 mg/ml Polybrene was added. MDA-MB-231 shScrib or shLgl1 cells were infected with the viruses containing Lenti-Neon-Scrib or Lenti-Neon-Lgl1, respectively; 24 h postinfection, the medium was replaced with fresh

Oligonucleotides	Sequence 5'–3'
Forward oligo tet-shScrib	CCGGCTGGCCTGTGACTAACTAACTCTCGAGAGTTAGTTAGTCACAGGCCAGTTTTTG
Reverse oligo tet-shScrib	AATTCAAAAACTGGCCTGTGACTAACTAACTCTCGAGAGTTAGTTAGTCACAGGCCAG
Forward oligo tet-shLgl1	CCGGCCCTCACTTTGCAGAGTATTTCTCGAGAAATACTCTGCAAAGTGAGGGTTTTTG
Reverse oligo tet-shLgl1	AATTCAAAAACCCTCACTTTGCAGAGTATTTCTCGAGAAATACTCTGCAAAGTGAGGG

TABLE 2: Oligonucleotides used to create Tet-plko-shScrib and Tet-plko-shLgl1.

medium. Neon positive cells were isolated by sorting using BD FACSAria III.

Immunoprecipitation assay of endogenous proteins

MDA-MB-231 cells were grown in a 100-mm dish to 90% confluency. Cells were harvested with 800 μl NP-40 buffer (20 mM Tris, pH = 8.0, 150–200 mM NaCl, 0.5 mM EDTA, 1% NP-40, 1 mM DTT, 5% Glycerol and Protease inhibitor cocktail; Sigma-Aldrich). Cell extracts were sonicated and centrifuged at 4°C for 15 min at $16,000 \times g$. The appropriate antibodies were incubated with cell lysate on a rotator at 4°C for 2 h. The lysate-antibodies mix was added to A/G beads or protein L beads (for IP with anti-Scrib) (Santa Cruz Biotechnologies) prewashed with 300 μl NP-40 buffer and incubated on a rotator at 4°C for 2 h. Then, the mix was washed three times with NP-40 Buffer and SDS-sample buffer was added. Samples were dissolved on SDS–PAGE and analyzed by Western blot. Proteins from Western blots were detected using the EZ-ECL Chemiluminescence Detection kit (Biological Industries) and the band intensity was analyzed using Bio-Rad Gel dox CR Luminescent Image Analyzer and Fujifilm Image Gauge Ver. 3.46 software (Fujifilm, Tokyo, Japan). The ImageGauge software detects saturation ensuring the linearity of the signal.

Coimmunoprecipitation assay

HEK293T cells were grown in a 60-mm dish to 90% confluency. After 18 h, cells were transfected with 6 μg DNA per plate, mixed with 36 μg PEI in DMEM. Cells were harvested at 24–48 h posttransfection with 300 μl NP-40 Buffer (20 mM Tris pH = 8.0, 150–200 mM NaCl, 0.5 mM EDTA, 1% NP-40, 1 mM DTT, 5% Glycerol and Protease inhibitor cocktail; Sigama-Aldrich). Cell extracts were sonicated and centrifuged at 4°C for 15 min at $16,000 \times g$. The appropriate antibodies were incubated with protein A/G beads (Santa Cruz Biotechnologies) prewashed with 300 μl NP-40 buffer on a rotator at 4°C for 1.5–2 h. The beads-antibodies mix was washed three times with NP-40 buffer. The cell extracts were added to the bead-antibody mix and incubated on rotator at 4°C for 2 h. Then, the mix was washed three times with NP-40 buffer and SDS-sample buffer was added. Samples were dissolved on SDS–PAGE and analyzed by Western blot.

Wound scratch assay and immunofluorescence

Cells were seeded on coverslips coated with Collagen type I (Sigma-Aldrich). After 14 h, cells were washed once with fresh medium and three parallel scratches were performed using a small pipette tip. Cells were washed with phosphate-buffered saline (PBS and fresh medium was added, incubated for 4 h at 37°C in a humidified atmosphere of 5% CO_2 and 95% air. Then, cells were fixed with 4% formaldehyde in PBS for 15 min, washed three time with PBS, and permeabilized for 3 min with PBS containing 0.2% Triton X-100 and 0.5% bovine serum albumin (BSA). Cells were washed three times and blocked with horse serum diluted 1:50 for 35 min at 37°C. Cells were washed and incubated with primary antibodies in PBS containing 0.1% BSA for 2 h at 37°C or overnight at 4°C. Coverslips were washed three times and incubated with secondary antibodies in PBS containing 0.1% BSA for 1 h at RT. For DAPI staining, cells were incubated for 5 min at RT with 300 nM DAPI (Sigma-Aldrich). For Golgi apparatus staining, cells were incubated for 1 h with wheat germ agglutinin (Invitrogene) followed by staining with Alexa Fluor 555 conjugate (1:4000) (Invitrogen) as described above. Cover slips were mounted on slides (Thermo-Scientific) using Vectachield mounting medium (Vector Laboratories). Confocal images were obtained with Nikon Yokogawa W1 Spinning Disk. Line scans of Scrib, Lgl1, NMIIB, and aPKCζ were measured with ImageJ software package (National Institutes of Health, Bethesda, MD). For colocalization analysis, the PCC was calculated between the intensity profiles of Scrib, Lgl1, NMIIB, and aPKCz at the cell leading edge and at the lamella. The PCC was calculated using Excel (Microsoft) and Prism 6 (GraphPad). Statistical analysis was done using Prism 6. For Golgi polarization analysis, statistical analysis was done using Prism 6. Data were examined by ANOVA with a post hoc test between the groups.

For live imaging, 5×10^5 cells were seeded on μ-Slide 4 well-coated chamber (ibidi), one parallel scratch was performed in each well and after 3 h live cell imaging was carried out at 37°C with 5% CO2. Live images were taken every 10 min using Nikon Ti with Objective Plan-Apochromat 40×/1.40 Oil DIC M27. Movies were processed using ImageJ, and the paths of 10 randomly chosen cells were plotted for each experimental group. Speed and persistence of migration were extracted from the track plots. Statistical analysis was done using Prism 6. Data were examined by ANOVA with a post hoc test between the groups.

TX-100 solubility assay

The 1×10^6 cells were seeded on 30-mm dishes. After cell attachment, eight horizontal and eight vertical scratches were performed using a small pipette tip and the cells were incubated for 4 h. PEM buffer (200 μl; 100 mM PIPES, pH 6.9, 1 mM $MgCl_2$, 1 mM EGTA, 1% TX-100, and protease inhibitor mix cocktail; Sigma-Aldrich) was added to each plate and incubated on rotator for 15 min at 4°C. Triton soluble fractions were collected and centrifuged for 5 min at $16,000 \times g$ to remove the remnants of the insoluble fraction. Then the supernatants were transferred to fresh tubes and SDS–PAGE sample buffer was added. The insoluble fractions were washed with 300 μl ice-cold PEM buffer and dissolved in 150 μl SDS–PAGE sample buffer. All samples were incubated for 5 min at 90 °C and then separated on 8% SDS–PAGE and analyzed with Western blotting, and band intensity was analyzed as described above. To calculate the percentage of the proteins in the TX–100-insoluble fraction, the intensity of proteins in the Triton-soluble fraction was divided by the sum of the intensities of the proteins in the Triton-soluble and -insoluble fractions.

Adhesion assay

The 1.5×10^5 cells were seeded on 30-mm plates. At 1 h postseeding, cells were washed gently with PBS and high-glucose DMEM medium was added to the dishes .Phase-contrast images of randomly chosen fields were taken with Nikon Eclipse Ts2 at ×20. The percentage of adhered cells relative to total cells in each field was quantified using Excel and Prism 6. Statistical analysis was done using Prism 6. Data were examined by ANOVA with a post hoc test between the groups.

Polarity index

The 1×10^6 cells were seeded in a 6-well plate and wound scratch assay was performed as described above. After 4 h, phase-contrast images of randomly chosen fields were taken with Nikon Eclipse Ts2 at ×20. For each cell line, the PI was calculated by dividing the length of the migration axis (which denotes the direction of migration) by the length of the perpendicular axis passes by the centroid of the cell. Measurements were analyzed using ImageJ. Statistical analysis was done using Prism 6. Data were examined by two-tailed Student's t test between each group.

Focal adhesions and Immunofluorescence

The 1×10^6 cells were subjected to wound scratch assay, fixed, permeabilized, and blocked as described above. Cells were incubated

with anti-Paxillin antibodies in PBS containing 0.1% BSA overnight at 4°C. Cover slips were washed three times with PBS and Donkey anti-mouse conjugated to Cy3 was added and incubated for 1 h at RT. Cover slips were mounted as described above. Confocal images were obtained with Yokogawa W1 Nikon Spinning Disk 60×. Size of focal adhesions was analyzed using ImageJ (Horzum *et al.*, 2014) and Excel. Statistical analysis was done using Prism 6. Data were examined by ANOVA with a post hoc test between the groups.

Wound closure assay

Cells were subjected to wound scratch assay as described above. Images of the wound area were taken directly after wound was performed (0 h), after 6 h, and after 15 h with Nikon Eclipse Ts2 at ×4. The exact location of the image within the monolayer was marked to identify the same gap over the next 15 h. Images were analyzed using ImageJ, gap distances of the scratch between one side and the other were measured alongside the wound at 10 different points per gap. The mean of the measured distances was then calculated and compared with the mean distance of the gap at the starting time point of the experiment. Statistical analysis was done using Excel and Prism 6. Data were examined by ANOVA with a post hoc test between the groups.

REFERENCES

Assemat E, Bazellieres E, Pallesi-Pocachard E, Le Bivic A, Massey-Harroche D (2008). Polarity complex proteins. Biochim Biophys Acta 1778, 614–630.

Audebert S, Navarro C, Nourry C, Chasserot-Golaz S, Lecine P, Bellaiche Y, Dupont JL, Premont RT, Sempere C, Strub JM, et al. (2004). Mammalian Scribble forms a tight complex with the betaPIX exchange factor. Curr Biol 14, 987–995.

Bailey MJ, Prehoda KE (2015). Establishment of par-polarized cortical domains via phosphoregulated membrane motifs. Dev Cell 35, 199–210.

Betapudi V, Licate LS, Egelhoff TT (2006). Distinct roles of nonmuscle myosin II isoforms in the regulation of MDA-MB-231 breast cancer cell spreading and migration. Cancer Res 66, 4725–4733.

Betschinger J, Eisenhaber F, Knoblich JA (2005). Phosphorylation-induced autoinhibition regulates the cytoskeletal protein Lethal (2) giant larvae. Curr Biol 15, 276–282.

Bilder D (2004). Epithelial polarity and proliferation control: links from the Drosophila neoplastic tumor suppressors. Genes Dev 18, 1909–1925.

Bilder D, Li M, Perrimon N (2000). Cooperative regulation of cell polarity and growth by Drosophila tumor suppressors. Science 289, 113–116.

Bilder D, Perrimon N (2000). Localization of apical epithelial determinants by the basolateral PDZ protein Scribble. Nature 403, 676–680.

Bilder D, Schober M, Perrimon N (2003). Integrated activity of PDZ protein complexes regulates epithelial polarity. Nat Cell Biol 5, 53–58.

Bonello TT, Peifer M (2019). Scribble: A master scaffold in polarity, adhesion, synaptogenesis, and proliferation. J Cell Biol 218, 742–756.

Caria S, Magtoto CM, Samiei T, Portela M, Lim KYB, How JY, Stewart BZ, Humbert PO, Richardson HE, Kvansakul M (2018). Drosophila melanogaster Guk-holder interacts with the Scribbled PDZ1 domain and regulates epithelial development with Scribbled and Discs Large. J Biol Chem 293, 4519–4531.

Cau J, Hall A (2005). Cdc42 controls the polarity of the actin and microtubule cytoskeletons through two distinct signal transduction pathways. J Cell Sci 118, 2579–2587.

Conti MA, Adelstein RS (2008). Nonmuscle myosin II moves in new directions. J Cell Sci 121, 11–18.

Dahan I, Petrov D, Cohen-Kfir E, Ravid S (2014). The tumor suppressor Lgl1 forms discrete complexes with NMII-A and Par6alpha-aPKCzeta that are affected by Lgl1 phosphorylation. J Cell Sci 127, 295–304.

Dahan I, Yearim A, Touboul Y, Ravid S (2012). The tumor suppressor Lgl1 regulates NMII-A cellular distribution and focal adhesion morphology to optimize cell migration. Mol Biol Cell 23, 591–601.

Daulat AM, Puvirajesinghe TM, Camoin L, Borg JP (2018). Mapping cellular polarity networks using mass spectrometry-based strategies. J Mol Biol 430, 3545–3564.

Dong W, Zhang X, Liu W, Chen YJ, Huang J, Austin E, Celotto AM, Jiang WZ, Palladino MJ, Jiang Y, et al. (2015). A conserved polybasic domain mediates plasma membrane targeting of Lgl and its regulation by hypoxia. J Cell Biol 211, 273–286.

Dow LE, Kauffman JS, Caddy J, Zarbalis K, Peterson AS, Jane SM, Russell SM, Humbert PO (2007). The tumour-suppressor Scribble dictates cell polarity during directed epithelial migration: regulation of Rho GTPase recruitment to the leading edge. Oncogene 26, 2272–2282.

Dulyaninova NG, Malashkevich VN, Almo SC, Bresnick AR (2005). Regulation of myosin-IIA assembly and Mts1 binding by heavy chain phosphorylation. Biochemistry 44, 6867–6876.

Elsum IA, Martin C, Humbert PO (2013). Scribble regulates an EMT polarity pathway through modulation of MAPK-ERK signaling to mediate junction formation. J Cell Sci 126, 3990–3999.

Elsum I, Yates L, Humbert PO, Richardson HE (2012). The Scribble-Dlg-Lgl polarity module in development and cancer: from flies to man. Essays Biochem 53, 141–168.

Etienne-Manneville S, Hall A (2001). Integrin-mediated activation of Cdc42 controls cell polarity in migrating astrocytes through PKCzeta. Cell 106, 489–498.

Even-Faitelson L, Ravid S (2006). PAK1 and aPKCzeta regulate myosin II-B phosphorylation: a novel signaling pathway regulating filament assembly. Mol Biol Cell 17, 2869–2881.

Feigin ME, Akshinthala SD, Araki K, Rosenberg AZ, Muthuswamy LB, Martin B, Lehmann BD, Berman HK, Pietenpol JA, Cardiff RD, Muthuswamy SK (2014). Mislocalization of the cell polarity protein scribble promotes mammary tumorigenesis and is associated with basal breast cancer. Cancer Res 74, 3180–3194.

Frank SR, Hansen SH (2008). The PIX-GIT complex: a G protein signaling cassette in control of cell shape. Semin Cell Dev Biol 19, 234–244.

Golomb E, Ma X, Jana SS, Preston YA, Kawamoto S, Shoham NG, Goldin E, Conti MA, Sellers JR, Adelstein RS (2004). Identification and characterization of nonmuscle myosin II-C, a new member of the myosin II family. J Biol Chem 279, 2800–2808.

Gomes ER, Jani S, Gundersen GG (2005). Nuclear movement regulated by Cdc42, MRCK, myosin, and actin flow establishes MTOC polarization in migrating cells. Cell 121, 451–463.

Gupton SL, Waterman-Storer CM (2006). Spatiotemporal feedback between actomyosin and focal-adhesion systems optimizes rapid cell migration. Cell 125, 1361–1374.

Hiroyasu S, Stimac GP, Hopkinson SB, Jones JCR (2017). Loss of beta-PIX inhibits focal adhesion disassembly and promotes keratinocyte motility via myosin light chain activation. J Cell Sci 130, 2329–2343.

Horzum U, Ozdil B, Pesen-Okvur D (2014). Step-by-step quantitative analysis of focal adhesions. MethodsX 1, 56–59.

Humbert PO, Dow LE, Russell SM (2006). The Scribble and Par complexes in polarity and migration: friends or foes? Trends Cell Biol 16, 622–630.

Humbert PO, Grzeschik NA, Brumby AM, Galea R, Elsum I, Richardson HE (2008). Control of tumourigenesis by the Scribble/Dlg/Lgl polarity module. Oncogene 27, 6888–6907.

Humphries JD, Byron A, Bass MD, Craig SE, Pinney JW, Knight D, Humphries MJ (2009). Proteomic analysis of integrin-associated complexes identifies RCC2 as a dual regulator of Rac1 and Arf6. Sci Signal 2, ra51.

Kallay LM, McNickle A, Brennwald PJ, Hubbard AL, Braiterman LT (2006). Scribble associates with two polarity proteins, Lgl2 and Vangl2, via distinct molecular domains. J Cell Biochem 99, 647–664.

Klezovitch O, Fernandez TE, Tapscott SJ, Vasioukhin V (2004). Loss of cell polarity causes severe brain dysplasia in Lgl1 knockout mice. Genes Dev 18, 559–571.

Kolega J (1998). Cytoplasmic dynamics of myosin IIA and IIB: spatial 'sorting' of isoforms in locomoting cells. J Cell Sci 111, 2085–2095.

Kuo JC, Han X, Hsiao CT, Yates JR 3rd, Waterman CM (2011). Analysis of the myosin-II-responsive focal adhesion proteome reveals a role for beta-Pix in negative regulation of focal adhesion maturation. Nat Cell Biol 13, 383–393.

Kuphal S, Wallner S, Schimanski CC, Bataille F, Hofer P, Strand S, Strand D, Bosserhoff AK (2006). Expression of Hugl-1 is strongly reduced in malignant melanoma. Oncogene 25, 103–110.

Lo CM, Buxton DB, Chua GC, Dembo M, Adelstein RS, Wang YL (2004). Nonmuscle myosin IIb is involved in the guidance of fibroblast migration. Mol Biol Cell 15, 982–989.

Martin-Belmonte F, Perez-Moreno M (2012). Epithelial cell polarity, stem cells and cancer. Nat Rev Cancer 12, 23–38.

Mathew D, Gramates LS, Packard M, Thomas U, Bilder D, Perrimon N, Gorczyca M, Budnik V (2002). Recruitment of scribble to the synaptic scaffolding complex requires GUK-holder, a novel DLG binding protein. Curr Biol 12, 531–539.

Michaelis UR, Chavakis E, Kruse C, Jungblut B, Kaluza D, Wandzioch K, Manavski Y, Heide H, Santoni MJ, Potente M, et al. (2013). The polarity protein Scrib is essential for directed endothelial cell migration. Circ Res 112, 924–934.

Moreira S, Morais-de-Sa E (2016). Spatiotemporal phosphoregulation of Lgl: Finding meaning in multiple on/off buttons. Bioarchitecture 6, 29–38.

Murakami N, Kotula L, Hwang Y-W (2000). Two distinct mechanisms for regulation of nonmuscle myosin assembly via the heavy chain: Phosphorylation for MIIB and Mts 1 binding for MIIA. Biochemistry 39, 11441–11451.

Nabi IR (1999). The polarization of the motile cell. J Cell Sci 112 (Pt 12), 1803–1811.

Nola S, Sebbagh M, Marchetto S, Osmani N, Nourry C, Audebert S, Navarro C, Rachel R, Montcouquiol M, Sans N, et al. (2008). Scrib regulates PAK activity during the cell migration process. Hum Mol Genet 17, 3552–3565.

Osmani N, Vitale N, Borg JP, Etienne-Manneville S (2006). Scrib controls Cdc42 localization and activity to promote cell polarization during astrocyte migration. Curr Biol 16, 2395–2405.

Parsons JT, Horwitz AR, Schwartz MA (2010). Cell adhesion: integrating cytoskeletal dynamics and cellular tension. Nat Rev Mol Cell Biol 11, 633–643.

Pearson HB, Perez-Mancera PA, Dow LE, Ryan A, Tennstedt P, Bogani D, Elsum I, Greenfield A, Tuveson DA, Simon R, Humbert PO (2011). SCRIB expression is deregulated in human prostate cancer, and its deficiency in mice promotes prostate neoplasia. J Clin Invest 121, 4257–4267.

Phillips CL, Yamakawa K, Adelstein RS (1995). Cloning of the cDNA encoding human nonmuscle myosin heavy chain-B and analysis of human tissues with isoform-specific antibodies. J Muscle Res Cell Motil 16, 379–389.

Pires HR, Boxem M (2018). Mapping the Polarity Interactome. J Mol Biol 430, 3521–3544.

Plant PJ, Fawcett JP, Lin DC, Holdorf AD, Binns K, Kulkarni S, Pawson T (2003). A polarity complex of mPar-6 and atypical PKC binds, phosphorylates and regulates mammalian Lgl. Nat Cell Biol 5, 301–308.

Raab M, Swift J, Dingal PC, Shah P, Shin JW, Discher DE (2012). Crawling from soft to stiff matrix polarizes the cytoskeleton and phosphoregulates myosin-II heavy chain. J Cell Biol 199, 669–683.

Ridley AJ, Schwartz MA, Burridge K, Firtel RA, Ginsberg MH, Borisy G, Parsons JT, Horwitz AR (2003). Cell migration: integrating signals from front to back. Science 302, 1704–1709.

Ronen D, Ravid S (2009). Myosin II tailpiece determines its paracrystal structure, filament assembly properties, and cellular localization. J Biol Chem 284, 24948–24957.

Rosenberg M, Ravid S (2006). Protein kinase Cg regulates myosin IIB phosphorylation, cellular localization, and filament assembly. Mol Biol Cell 17, 1364–1374.

Schimanski CC, Schmitz G, Kashyap A, Bosserhoff AK, Bataille F, Schafer SC, Lehr HA, Berger MR, Galle PR, Strand S, Strand D (2005). Reduced expression of Hugl-1, the human homologue of Drosophila tumour suppressor gene lgl, contributes to progression of colorectal cancer. Oncogene 24, 3100–3109.

Shohet RV, Conti MA, Kawamoto S, Preston YA, Brill DA, Adelstein RS (1989). Cloning of the cDNA encoding the myosin heavy chain of a vertebrate cellular myosin. Proc Natl Acad Sci USA 86, 7726–7730.

Simons M, Wang M, McBride OW, Kawamoto S, Yamakawa K, Gdula D, Adelstein RS, Weir L (1991). Human nonmuscle myosin heavy chains are encoded by two genes located on different chromosomes. Circ Res 69, 530–539.

Stephens R, Lim K, Portela M, Kvansakul M, Humbert PO, Richardson HE (2018). The scribble cell polarity module in the regulation of cell signaling in tissue development and tumorigenesis. J Mol Biol 430, 3585–3612.

Strand D, Jakobs R, Merdes G, Neumann B, Kalmes A, Heid HW, Husmann I, Mechler M (1994a). The Drosophila lethal(2)giant larvae tumor suppressor protein forms homo-oligomers and is associated with nonmuscle myosin II heavy chain. J Cell Biol 127, 1361–1373.

Strand D, Raska I, Mechler BM (1994b). The Drosophila lethal(2)giant larvae tumor suppressor protein is a component of the cytoskeleton. J Cell Biol 127, 1345–1360.

Szafranski P, Goode S (2007). Basolateral junctions are sufficient to suppress epithelial invasion during Drosophila oogenesis. Dev Dyn 236, 364–373.

Tanentzapf G, Tepass U (2003). Interactions between the crumbs, lethal giant larvae and bazooka pathways in epithelial polarization. Nat Cell Biol 5, 46–52.

ten Klooster JP, Jaffer ZM, Chernoff J, Hordijk PL (2006). Targeting and activation of Rac1 are mediated by the exchange factor beta-Pix. J Cell Biol 172, 759–769.

Thomas DG, Yenepalli A, Denais CM, Rape A, Beach JR, Wang YL, Schiemann WP, Baskaran H, Lammerding J, Egelhoff TT (2015). Non-muscle myosin IIB is critical for nuclear translocation during 3D invasion. J Cell Biol 210, 583–594.

Vicente-Manzanares M, Choi CK, Horwitz AR (2009a). Integrins in cell migration—the actin connection. J Cell Sci 122, 199–206.

Vicente-Manzanares M, Koach MA, Whitmore L, Lamers ML, Horwitz AF (2008). Segregation and activation of myosin IIB creates a rear in migrating cells. J Cell Biol 183, 543–554.

Vicente-Manzanares M, Ma X, Adelstein RS, Horwitz AR (2009b). Non-muscle myosin II takes centre stage in cell adhesion and migration. Nat Rev Mol Cell Biol 10, 778–790.

Vicente-Manzanares M, Newell-Litwa K, Bachir AI, Whitmore LA, Horwitz AR (2011). Myosin IIA/IIB restrict adhesive and protrusive signaling to generate front-back polarity in migrating cells. J Cell Biol 193, 381–396.

Vicente-Manzanares M, Zareno J, Whitmore L, Choi CK, Horwitz AF (2007). Regulation of protrusion, adhesion dynamics, and polarity by myosins IIA and IIB in migrating cells. J Cell Biol 176, 573–580.

Wen W, Zhang M (2018). Protein complex assemblies in epithelial cell polarity and asymmetric cell division. J Mol Biol 430, 3504–3520.

Yu HW, Chen YQ, Huang CM, Liu CY, Chiou A, Wang YK, Tang MJ, Kuo JC (2015). beta-PIX controls intracellular viscoelasticity to regulate lung cancer cell migration. J Cell Mol Med 19, 934–947.

Zhan L, Rosenberg A, Bergami KC, Yu M, Xuan Z, Jaffe AB, Allred C, Muthuswamy SK (2008). Deregulation of scribble promotes mammary tumorigenesis and reveals a role for cell polarity in carcinoma. Cell 135, 865–878.

Zhao ZS, Manser E, Loo TH, Lim L (2000). Coupling of PAK-interacting exchange factor PIX to GIT1 promotes focal complex disassembly. Mol Cell Biol 20, 6354–6363.

Zhu J, Shang Y, Wan Q, Xia Y, Chen J, Du Q, Zhang M (2014). Phosphorylation-dependent interaction between tumor suppressors Dlg and Lgl. Cell Res 24, 451–463.